Journal of Earth Science, *Vol. 34*, *No. 3*, *p. 879−899*, *June 2023* *ISSN 1674-487X*
Printed in China
https://doi.org/10.1007/s12583-021-1540-x

Early Cretaceous Tectonostratigraphic Evolution of the Southern Tunisian Margin Based on Gravity, Seismic and Potential Field Data: New Insights into a Geodynamic Evolution in a Tethyan and Mesogean Rifting Context

Mohamed Ben Chelbi *

Faculty of Sciences of Tunis, *Laboratory of Geodynamic*, *Geonumeric and Geomaterials* (*L3G*) *LR18ES37*, *University of Tunis El Manar*, *Tunis*, *Tunisia*

Mohamed Ben Chelbi: https://orcid.org/0000-0002-1699-0091

ABSTRACT: Many geophysical and geological data have been used to interpret the tectonic evolution of the south-eastern part of the Tunisian margin and to analyze the dominant structures in the area. The Menzel Habib Plain (MHP) and surroundings, targeted by this study, exhibits thick siliciclastic and carbonate formations attributed to the Early Cretaceous period. Integration of seismic and gravimetric data coupled with analysis of the syndepositional faults affecting these formations prove that the Tunisian margin is dominated, during this period, by N-S to NE-SW extensional directions. The geodynamic evolution of the MHP is mainly due to the irregular normal movement of the N-S faults, which represents the southernmost branch of the N-S Axis (NSA) and of the NW-SE faults, which constitutes the SE segment of the South Atlasic fault corridor (SAFC). In addition, the NE-SW and E-W oriented faults contributed to this evolution. Over extensive periods, this network of faults determines horst and grabens basin geometry or tilted blocks inducing formation of several distinct areas with different subsidence rates. Simultaneously, the normal activity of the major faults promotes the vertical mobilization of the Triassic salt resulting in the individualization of several diapiric bodies, some of which pierced their sedimentary cover. These dynamics reflect echoes of the sinistral drifting of Africa with respect to Europe, integrated in a long Tethyan rifting cycle, and the beginning of opening of the Mesogean Sea, respectively.

KEY WORDS: Tunisian margin, Early Cretaceous, extensive tectonics, Tethyan and Mesogean rifting, geodynamics.

0 INTRODUCTION

The Tunisian Atlas, an eastward extension of the Maghrebide chain (Fig. 1a) (Raulin et al., 2011; Bodin et al., 2010; Guiraud et al., 2005; Piqué et al., 2002; Doglioni et al., 1994), has a record of long polyphase tectono-sedimentary evolution of the North African margin (Ben Chelbi, 2021; Ben Chelbi et al., 2008; Zouari et al., 1999; Piqué et al., 1998). Since the initial breakup of Pangea, the Tethys and Mesogean rifting periods (Min and Hou, 2019; Handy et al., 2010), and through the collision events that continue (Ghedhoui et al., 2016; Rosenbaum, 2014), the basin evolution has recorded tectono-sedimentary systems with complex facies and structures. Geological work that has targeted at the Tunisian margin indicated that this complexity is mainly due to a direct interaction between faulting, shown by the different networks of faults, and the sedimentation (Ben Chelbi, 2021; Ghanmi et al., 2017; Ben Chelbi et al., 2013, 2006; Gharbi et al., 2013; Masrouhi et al., 2008; Khomsi et al., 2006; Zouaghi et al., 2005). The Menzel Habib Plain (MHP), constituting the south-eastern termination of the Tunisian Atlas (Fig. 1b), was not spared from this tectono-sedimentary interaction. The plain is characterized by a range of stratigraphic and structural interference between all the major structures of the Tunisian margin (Fig. 1b). It occupies a central position between the Eastern Platform, the central Tunisian Atlas, the southern Atlas and the Jeffara (Fig. 1b). Geodynamically, the evolution of this zone is closely controlled by the irregular movements of the North-South Axis (NSA) and the South Atlasic fault corridor (SAFC) represented by the Hadhifa fault (Fig. 1c). Because of its complex structural and stratigraphic position, the MHP is of vital importance, both structurally and geodynamically, to understanding the larger neighboring structures evolved by major faults and the fault blocks. Although the geological position of the Menzel Habib Plain is very important, studies about this area are very rare and have only focused on mapping the various stratigraphic and structural units.

*Corresponding author: med.benchelbi@gmail.com

Manuscript received June 19, 2021.
Manuscript accepted September 9, 2021.

Ben Chelbi Mohamed, 2023. Early Cretaceous Tectonostratigraphic Evolution of the Southern Tunisian Margin Based on Gravity, Seismic and Potential Field Data: New Insights into a Geodynamic Evolution in a Tethyan and Mesogean Rifting Context. *Journal of Earth Science*, 34(3): 879–899. https://doi.org/10.1007/s12583-021-1540-x. http://en.earth-science.net

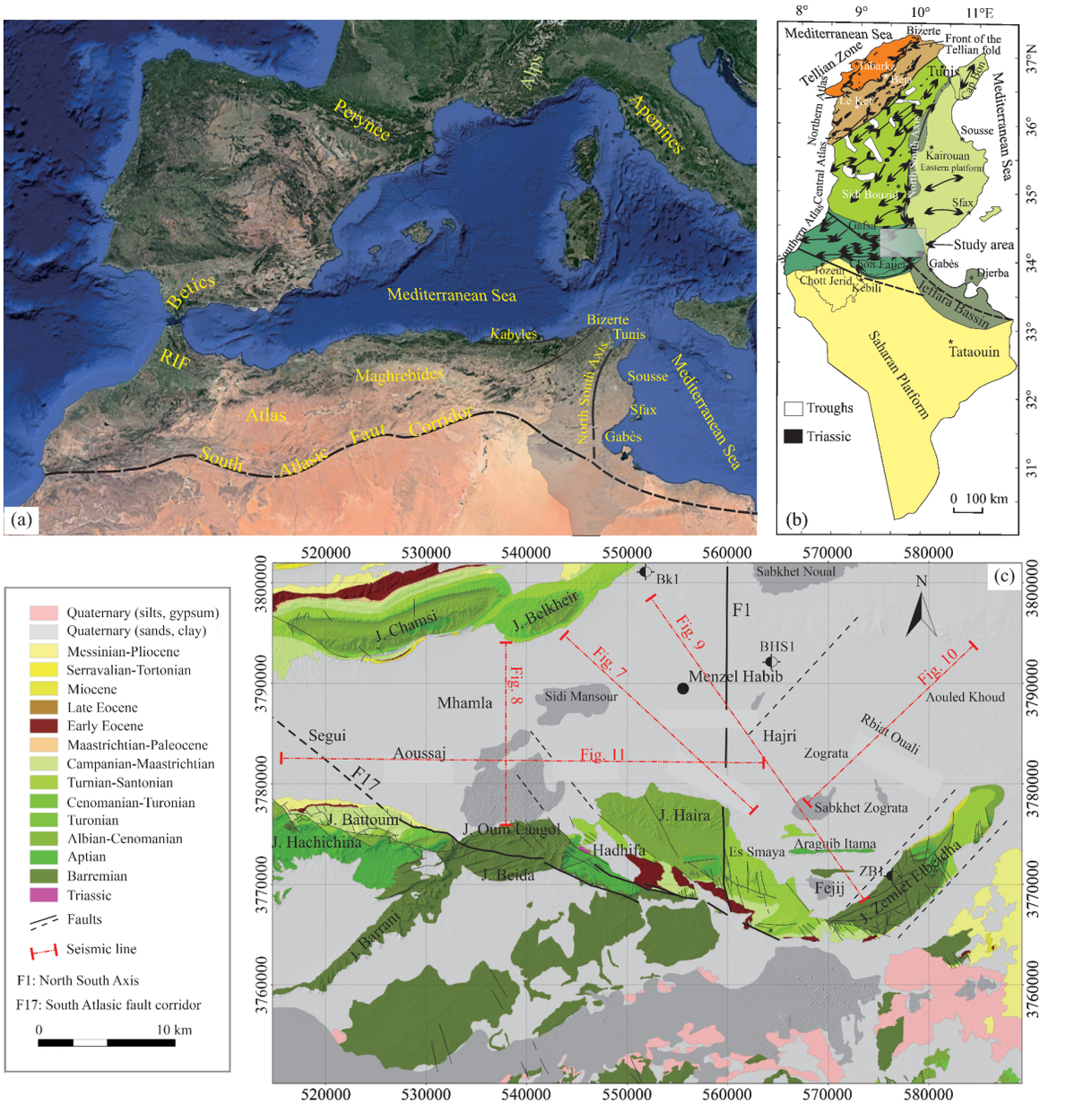

Figure 1. Geological context of the study area. (a) General position of the Tunisian margin in the Mediterranean context; (b) structural zoning of Tunisia (Ben Chelbi et al., 2008) showing the structural position of the study area in relation with the major structures of the central and southern Atlas, the eastern platform and the Tunisian Jeffara; (c) geological map of the study area showing the most master faults (F1 and F17) which affect the Menzel Habib Plain (MHP) and the position of the various seismic lines used in this study.

The study aims to: (1) determine the different fault networks that affect the study area; (2) study the tectono-sedimentary evolution of the study area in relation to the major fault systems based on field and subsurface data; (3) define and characterize links between the evolutionary model of the MHP and the neighboring regions of the Tunisian margin; (4) correlate the evolution of this zone with the tectonic events of Mediterranean chains resulted from general displacement of African and Eurasian plates.

1 DATA AND METHODOLOGY

The study of the deep structural architecture of the MHP and neighboring geological structures is inferred from interpretation of gravimetric data and seismic sections while the evolutionary geodynamic model of this zone is based on lithostratigraphic correlations carried out from petroleum wells and field investigations. Seismic sections were obtained from the Tunisian Petroleum Company (ETAP). The W1 petroleum well is used to show the succession of different stratigraphic sequences characterizing the trough using time-depth conversion of lithological data. Several seismic lines are interpreted to establish the main oriented faults which participated, firstly, to the facies development during sedimentation periods, and secondly to the final structuring of the study area, during compressive times. Gravimetric data were obtained by the Ministry of Agriculture acquired during 2016. The gravimetric campaign comprised 461 measurements distributed over a regular mesh covering the study area.

The geodynamic evolution of the MHP is interpreted, first, through the analysis of vertical facies and thickness variations of the Lower Cretaceous series on both sides of the NW-SE, E-W, NE-SW and N-S oriented faults and, secondly, through analysis of the main syndepositional faults affecting these formations. These fault plane directions and senses of slips were subsequently analyzed using FaultKinWin, Version 1.1 program. Since the Earliest Cretaceous, sedimentation has been largely controlled by this network of faults, in which we note a large variation of facies and thicknesses. Four petroleum wells were used to show the succession of stratigraphic sequences characterizing the plain, using time-depth conversion of lithological data to correlate the Lower Cretaceous formations on both sides of the major faults that characterize the study area. Interpretation of the both surface and subsurface data contributed to outline a general tectonic sketch of the study area into a global geodynamic setting during the Early Cretaceous period.

2 GEOLOGICAL FRAMEWORK

2.1 Lithostratigraphy

The stratigraphic series outcropping in the study area are essentially of Triassic, Cretaceous and Paleogene ages. The major part of this study zone is occupied by Quaternary deposits (Figs. 1c and 2). Triassic beds outcrop in Jebel Hadhifa, composed of clay, marl, limestone, gypsum, salt, anhydrite and sand. The Triassic Germanic facies, typical of the Tunisian margin, is evident. The only Lower Cretaceous outcrop is at the top part of the Bou Hedma, Sidi Aich and Orbata formations. The BHS, ZB1, BK1 and MAN1 oil wells characterizing the MHP and surroundings (Fig. 1c) served to study buried formations. The Melloussi Formation, 200 m thick, comprises interbedded sandstones and claystone with minor dolomite and anhydrite. This formation, has been deposited on a shallow marine shelf, with irregular subsidence. The Boudinar Formation is made up of white sand, fine to coarse grained, with fine interbedded levels of green shale, and occasionally thin levels of brown dolomite. The average thickness of this formation is 180 m. These two formations constitute the Sened Group which is largely described in the surrounding areas of Fejej Chott (Mejri et al., 2006). The Bou Hedma Formation, is essentially made up by claystones with interbedded sandstone, dolomite, limestone gypsum and occasional coal. The formation comprises 100 to 150 m of fine white sands which is characteristically found at the top of this formation, and is finally topped with 3 m of red dolomite forming a boundary between the Bou Hedma and the Sidi Aich Formation. At the core of Zemlet Elbeidha anticline, the Bouhedma Formation is represented by 1 250 m of alternating gypsum, claystone, sandstone and dolomite (Fig. 2) of which 800 m are penetrated the ZB1 petroleum well. The Sidi Aich Formation is widely spread sandy unit in central, and southern Tunisia. In our study area, this formation is composed of interbedded sand and varicoloured claystone with occasional dolomite and rare traces of coal. The average thickness of the Sidi Aich Formation is around 80 m. This last is usually overlapped by 40 to 60 m of brown and massive dolomites attributed to the Orbata Formation. On the south-eastern flank of the Zemlet Elbeidha anticline, these dolomites are replaced by a bar of polygenic conglomerates formed by dolomite blocks embedded in a sandy and clayey matrix. These dolomites are capped with another dolomitic cliff outcrop constituting the base of the Zebbag Formation, with a major unconformity. Consequently, if the base of Orbata is approximately synchronous, the top is completely diachronous depending on the sedimentation of the upper members, the subsequent erosion and the onlaps of the following series (Mejri et al., 2006).

The Late Cretaceous, including Albian beds, is represented by the Zebbag Formation (Upper Albian to Cenomanian), the Aleg Formation (Turonian to Lower Campanian), and the Abiod Formation (Lower Campanian to Upper Maastrichtian) (Fig. 2). These formations are composed in the lower part of dolomitic, gypsum and clay alternations, in the middle part, of argillaceous and marly deposits, and dolomites and limestones, in the upper part.

The Early Eocene period is represented by a continental unit formed by conglomerates, red clay, lacustrine limestone, and caliche, defining the Early Eocene Bouloufa Formation. The Miocene signified by 60 m of white sands which characterize the Beglia Formation. The Quaternary consists of predominantly unconsolidated sand and conglomerates at the base overlain by red clays with crystalline gypsum. These deposits are very rare and generally occupy foothills areas.

Paleogeographically, deposits of the Melloussi and Boudinar formations reflect a deltaic regressive detritic body evolving to a deltaic progradation towards the north (M'Rabet et al., 1995). Deposits of Bouhedma, Sidi Aich and Orbata formations characterize transgressive sedimentation on a low slope substratum. Facies and thickness changes, of these formations, are due to the activities of the main faults acting during extensive epochs, contemporaneous with sedimentation and to the irregular halokinetic rises of Triassic salt bodies.

2.2 Structural Evolution

Since the Triassic period, the Tunisian margin has recorded all the echoes of the geodynamic evolution of the Tethyan domain and the resulting structures (Fig. 2). Indeed, from the first breakup stages of Pangea during the Early Triassic, a system of regional NS, NE-SW and NW-SE trending faults have broken the sedimentary floor into a mosaic blocks and expanses. From this period a rifting system was implemented, along these faults, in response to an extensive tectonics involving a N-S minimum stress. Evidence of the first stages of the Tethyan rifting is dated to the Jurassic-Barremian period (Sekatni et al., 2008; Boughdiri et al., 2006; Soussi, 2003; Morgan et al., 1998). This mechanism of opening continued until Barremian period (Fig. 2). A radical change occurred during the Aptian that is seen in the changing direction of elongation to become NE-SW (Melki et al., 2010; Ben Chelbi et al., 2008). This change in the extensional stress orientation is indicated by reactivation of the NW-SE-normal faults, which created several NE-SW and NW-SE basins (Ben Chelbi et al., 2013, 2008). These evolved during the following periods and controlled troughs of the central Tunisian Atlas (Ben Chelbi et al., 2013) and the major escarpment of the southern Tunisian Atlas and Jeffara zone (Bodin et al., 2010). Simultaneously, the Tunisian Atlas records intense halokinetic activity (Fig. 2) forming dia-

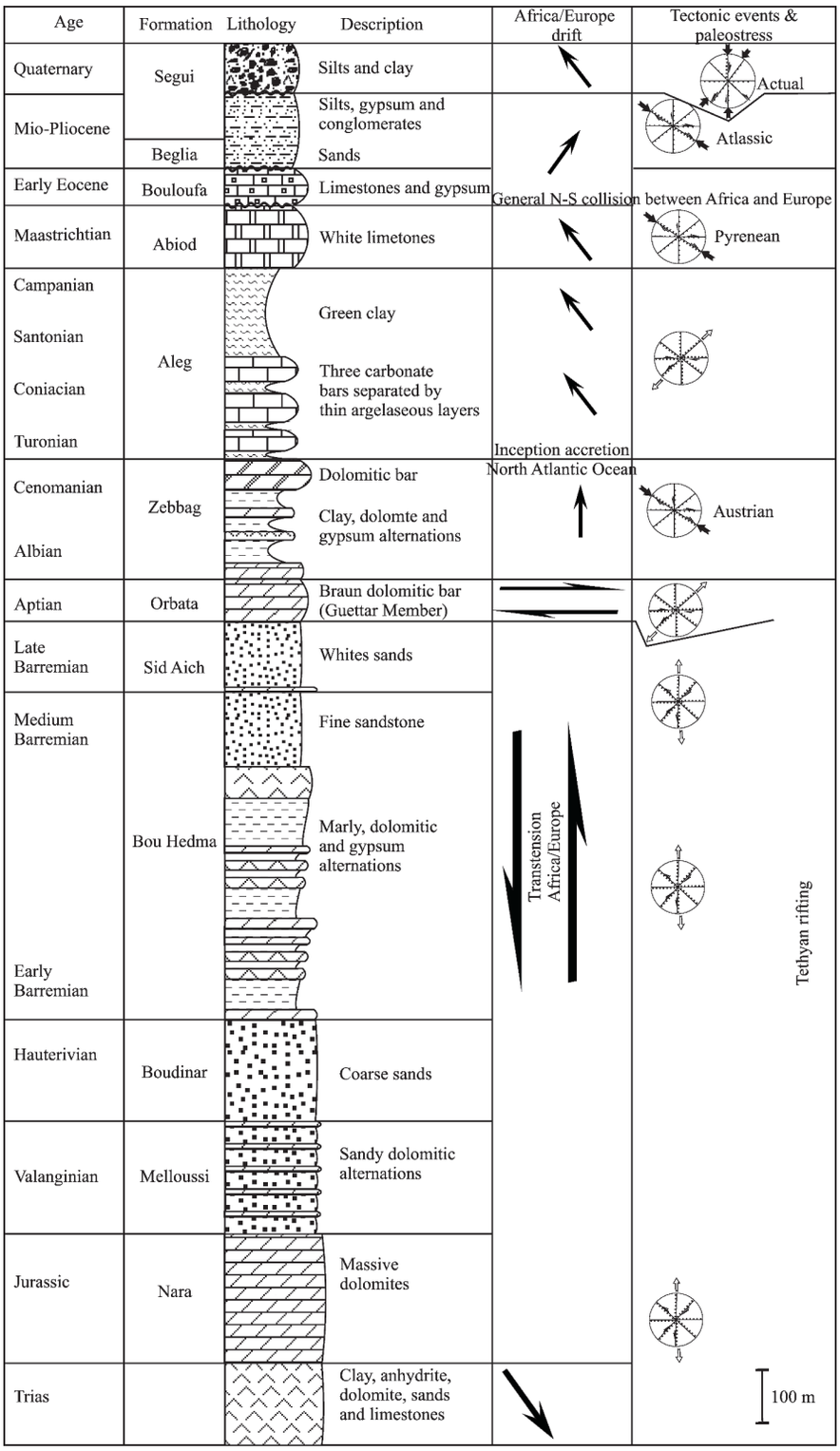

Figure 2. Geodynamic and stratigraphic context of the study area; columns 1, 2 and 3 show the different lithostratigraphic units outcropped or crossed by the various oil wells in the MHP; columns 4 and 5 expose the principal stages of Africa drifting with respect to Europe and the corresponding tectonic events recorded in the Tunisian margin since Triassic (modified after Ben Chelbi et al., 2013).

pirs and/or salt glaciers (Ben Chelbi et al., 2006; Vila et al., 1994).

The Tunisian margin was affected, during the Albian Cenomanian period, by compressive tectonics applying NW-SE maximum stress (Ben Chelbi, 2021) (Fig. 2). This dynamic has largely contributed to the moderate inversion of the different basins characterizing the Tunisian margin, the thrusting of the NE-SW Hercynian faults, the amplification of the subsidence on the NW-SE faults, the vertical rising of the saliferous Triassic series leading to the piercement of the cover and the

development of an angular unconformity on both limbs of the developed folds (Ben Chelbi, 2021).

During the Late Cretaceous the Tunisian margin was controlled by strike-slip faults (Ben Chelbi et al., 2008; Zouari et al., 1999), accompanied by reactivation of the north-south- , east-west- and NE-SW-trending normal faults with dextral component. The general inversion of the structures was recorded during the Middle Eocene (Ben Chelbi et al., 2013, 2006; Melki et al., 2010; Masrouhi et al., 2008) (Fig. 2). The first period of folding is assigned to the Tortonian (Tlig et al., 1991), whereas the ultimate compression leading to the building of the Tunisian Atlas Mountains began during the Villafranchian and has been continuing to the present day (Bouaziz et al., 2002; Fig. 2). This long period of compression controlled by NNW-SSE to N-S stress has contributed to the final configuration of the Tunisian Atlas in which NE-SW-, NW-SE-, E-W and N-S oriented faults were respectively reactivated with sinistral reverse, dextral reverse, reverse and sinistral slip. The southern Tunisian Atlas is no exception to this complex evolution. The actual architecture of this part of the Tunisian margin is characterized by coexistence of E-W trending folds which are truncated by NW-SE and N-S oriented major faults, representing the signature of the SAFC and NSA respectively. These faults have largely controlled sedimentation, over extensive periods, and caused the final structural geometry, during compressive epochs, of the southern Tunisian Atlas and the Jeffara escarpment.

3 GEOMORPHOLOGICAL AND HYDROLOGIC SETTING

Cartographically, the study area corresponds to a E-W oriented plain of low relief culminating to 150 m (Fig. 3). It is bounded on the north and south by two large orographic lines corresponding to the Jebel Chamsi-Jebel Belkhir and the northern chain of Chotts, respectively (Fig. 3). Jebel Berda constitutes the western limit of this plain. The MHP is drained by several wadis which flow in the Sabkhet Sidi Mansour, to the west, and in the Sabkhet Zograta and Sabkhet Ouled Khoud, to the east. The middle part of the MHP is shaped by two large topographic convexities, lengthened in a N-S and NE-SW direction. From west to east, the first high area is traced between Sabkhet Sidi Mansour and Garaet Hajri, while the second one lengthened the Bled et Teurbia (Fig. 3). These convexities constitute a dividing line of discharge of the various wadis. The first band corresponds to the layout of a N-S major fault which is passed by Jebel Es Smaya, to the south, and continues as far as Jebel Belkhir, to the north (Fig. 1c). The second convexity line represents the surface response of a deep NE-SW fault. This fault is seen by the rectilinearity of the source line of the wadis which diverge in Sabkhet Ouali. Oueds characterizing the western province flow either north in Sabkhet Noual or converge towards the Sebkhet Mhamla and Oued Rimth.

4 RESULTS

4.1 Gravity

4.1.1 Bouguer anomaly map

The Bouguer anomaly grid was established by adopting a process of interpolation of the minimum curvature. The Bouguer anomaly map expresses an amplitude of around 36 mGal, with values distributed between -42 and -6 mGal (Fig. 4). Gravimetric responses are characterized by long wavelength anomalies found in a decreasing gravimetric gradient from east to west. Surplus masses, reflecting the signature of positive density contrasts in relation to the density used in the Bouguer model, are organized in the eastern part of the study area (Fig. 4). A second zone characterized by surplus mass is also highlighted in the SW limit of the study zone. This subcircular geometry anomaly has a lower amplitude than those recorded in the eastern part of the area. The western part has a mass discrepancy with increasingly negative density contrasts towards the west (Fig. 4a). The recorded gravity gradient coincides with previ-

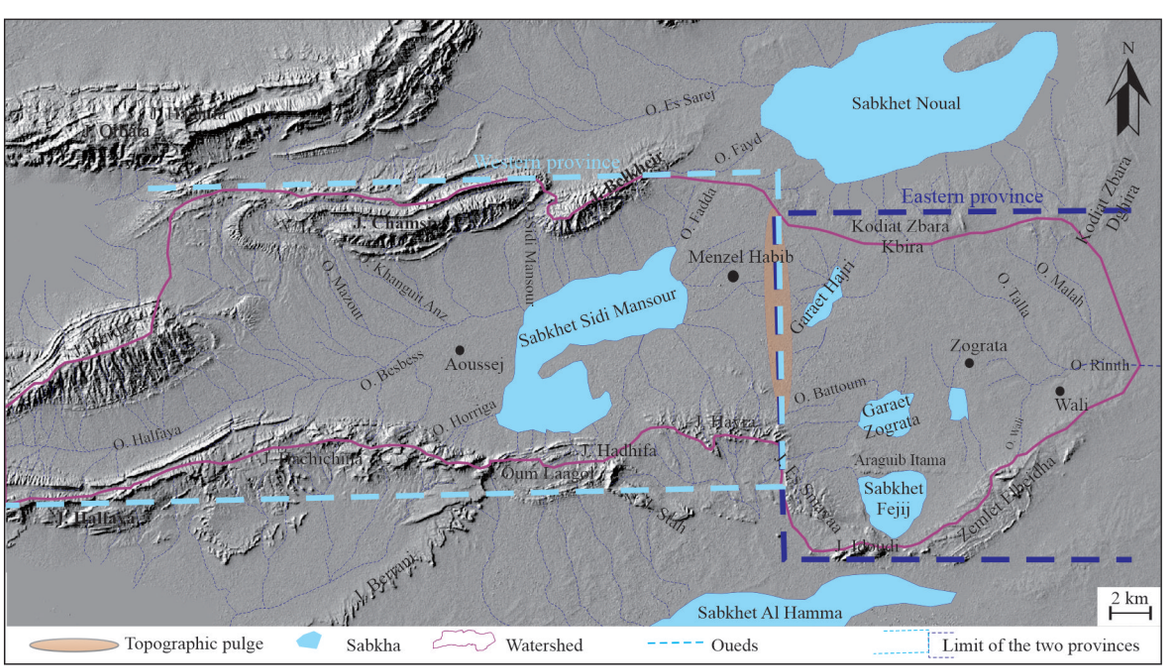

Figure 3. Morphologic and hydrographic context of the study area.

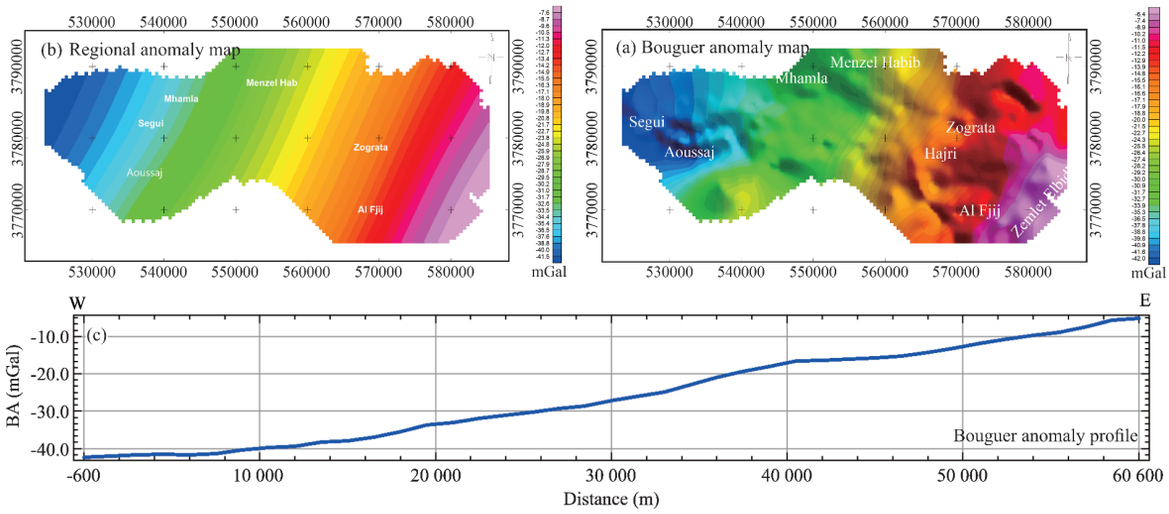

Figure 4. (a) Complete Bouguer gravity anomaly map of the Menzel Habib Plain; (b) regional gravity anomaly map; (c) E-W Bouguer anomaly profile of the study area.

ous regional scale work carried out in Tunisia (Fig. 4b). Thus the gravimetric work of Midassi (1982) reveals decreasing values of Bouguer anomaly towards the west (Figs. 4b and 4c). We also note that this trend can be explained by the geometry of the Moho discontinuity determined by the deep seismic carried out as part of the Geotraverse program (EGT project, 1990) which expresses a lithospheric deepening towards the Gafsa region.

4.1.2 Residual anomaly and contact modelling

The residual component was calculated by subtracting the low frequency anomalies from the total Bouguer anomaly. The map obtained offers a better characterization of the heterogeneities of local densities in the subsurface compared to the density of the Bouguer model. The residual component has emphasized gravimetric responses basins following short wavelength directions. The residual anomaly map (Fig. 5a) exposes that a clear N-S dividing line that differentiates the study area into two different large gravity provinces. In the western one, three basins are identified, accumulating thick series of low density rocks, characterizing the subsurface of Hajri, Mhamla and Segui. The negative anomaly typifying these E-W to ENE-WSW trending zones reaches a value of -3.8 mGal. Moreover, the eastern province comprises a dense substratum reflecting a positive anomaly. The Jebel Oum Laagol, Zemlet Elbeidha, Es Smayaa, Oued Zitoun and Rabiaat Ouali-Menzel Habib areas reach a value of 3.8 mGal and surround the Sabkhet Fejij area which shows a negative anomaly reaching a value of -4 mGal. The passage from the eastern province, with dense materials, towards the western one, is sudden and appears as a straight line defining the layout of the N-S major fault (Fig. 5a).

4.1.3 Structures and lineaments detection

To better understand the basins distribution, as well as the sedimentary series which compose them, we proceeded with the elaboration of the vertical derivative maps by accentuations of the gravimetric responses (Figs. 5b and 5c). The application of the first and second order vertical gradient is responsible for the accentuation of geological structures near the surface (Figs. 5b and 5c). These methods also make it possible to better separate the anomalies and to better specify the limits of the sources. A reduction in the complexity of gravity anomalies is clearly revealed through better localization of the extensions and geometries of the basins in the study area. The basins already revealed by the residual anomaly map are well expressed by the vertical gradient anomaly maps (Figs. 5b and 5c). The gravimetric signature of these basins shows a strong negative gradient which proves that these accumulation zones are occupied by low density sedimentary series. This response reflects the effects of a thick sand and clay series, attributed to the Mio-Plio-Quaternary time and the Lower Cretaceous period, which is characterized by a negative density contrast compared to the average density adopted by the model of Bouguer.

In order to determine the major directions of the different accumulation zones, already defined, we proceeded to the tilt angle derivative technique. This is widely used to define the limits of gravity sources (geological structures of interest located on the subsurface). Thus the limits of the sources are expressed by a zero angle. The tilt angle drift map reveals strong gravity gradients occupying the limits of the identified basins (Fig. 5d). The shown geometries are similar to that revealed by the first and second order vertical gradients maps.

Horizontal gradient filters are generally used to highlight lateral variations in density which may correspond to faults. This technique also makes it possible to characterize the major structural directions of the geological contacts. The latter is represented by gravimetric alignments which represent the maximum amplitude on the vertical gradient map. The interpretation of the maxima of the horizontal derivative thus made it possible to identify the discontinuities of density in the subsurface. These discontinuities are interpreted as the possible signatures of major fault systems across the region. The horizontal gradient map (Fig. 6a) clearly shows that the study area is differentiated into several sub-areas, each characterized by various structures and faults. A major N-S fault divides the study area into two provinces. That of the East is characterized by

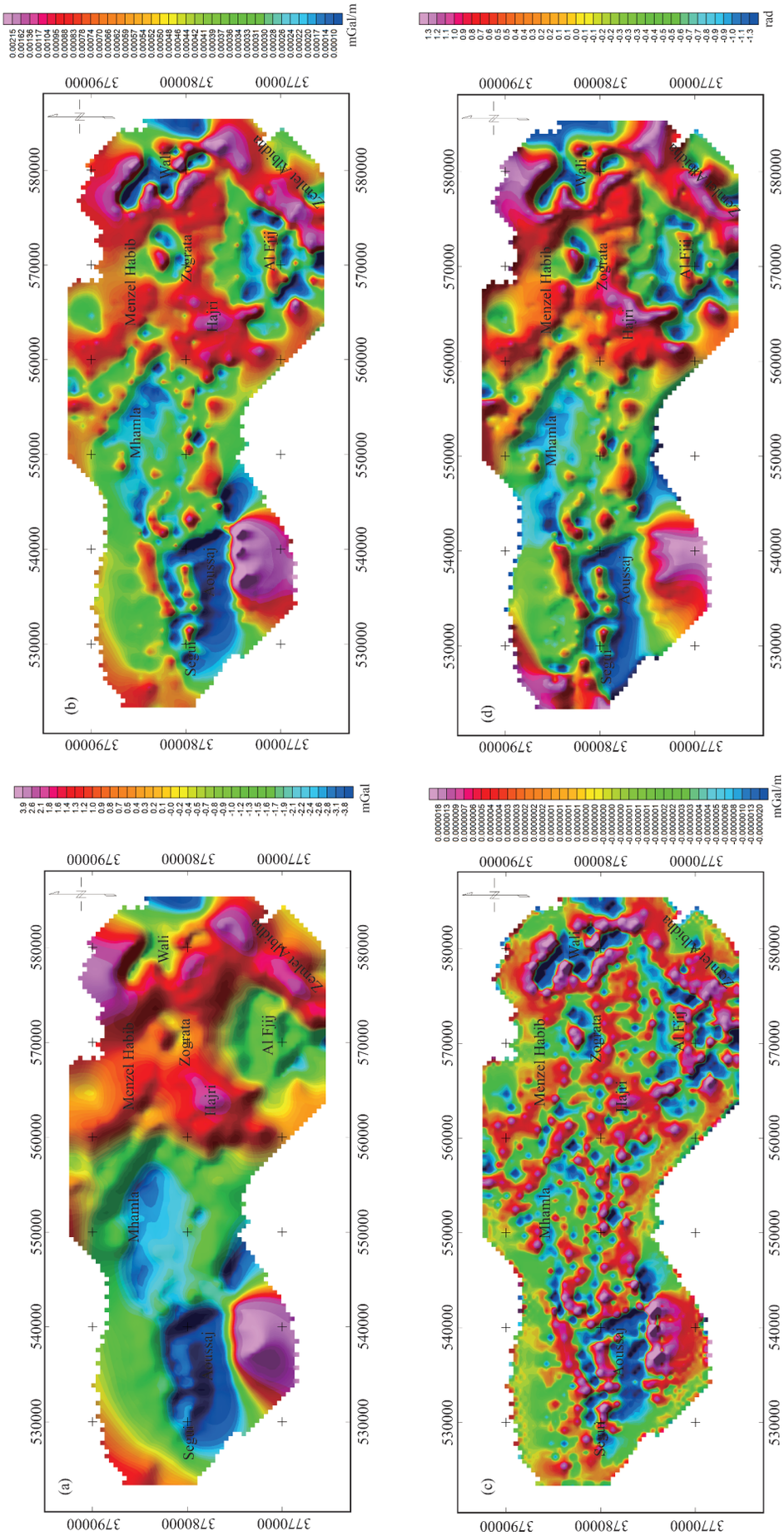

Figure 5. (a) Residual anomaly map of MHP; (b) and (c) vertical gradient anomaly maps; (d) tilt angle drift map.

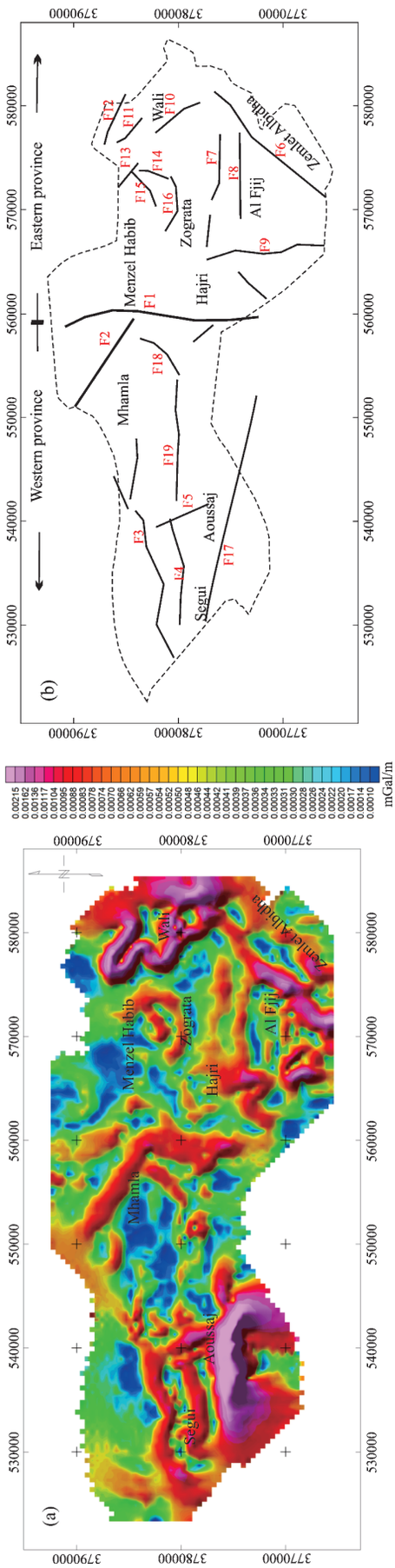

Figure 6. (a) Horizontal gradient map of the residual gravity anomaly data; (b) structural map deduced from compilation of data presented by the previous gravity maps.

NE-SW, E-W and NW-SE faults whereas the western province is affected by faults essentially oriented E-W.

The structural map obtained after application of these different techniques, shows several lineaments (Fig. 6b), which greatly contributed to the geodynamic evolution and the configuration of the MHP. The identified basins are orientated in two major directions. E-W basins characterize the western province of the study area, and NE-SW basins are identified in the neighborhood of Fejij and Zemlet Elbeidha.

The highlighted faults are distributed in the basement of Menzel Habib according to their amplitude and direction (Fig. 6b). The N-S fault, dividing the study area into two clear provinces and tracing west of Jebel Es Smayaa and passing through Oued Zitoun, is the most important one. This fault, called F1 (Fig. 6b) constitutes the prolongation, towards the south, of the mega N-S fault zone known as the North-South Axis. The Hadhifa fault, NW-SE direction, named F17 on the structural map (Fig. 6b), passing north of Jebel Oum Laagol, is of major importance in the deep structuring and the geodynamic evolution of MHP; it constitutes a segment of the SAFC.

The E-W faults are concentrated and essentially characterize the western province of the study area (Fig. 6b). The most important fault is that which divides this province into two sub-basins called the Mhamla and the Segui basins. The NE-SW and NW-SE faults characterize only the eastern province of the study area. This province is also controlled by N-S and E-W faults, the most important of which are those which break up the Fejij sub-basin. Figure 6, which shows the main faults that have been identified and affected the basement of Menzel Habib, demonstrates that the eastern province is intensely fractured compared to the western one.

4.2 Seismic Interpretation

To understand the deep architecture of the study area and highlight the role of the various faults in the geodynamic evolution of this area, several seismic sections have been interpreted. These sections, obtained from the Tunisian Petroleum Company (ETAP), are calibrated by the W1 well. The different seismic profiles used below are transversal to the average direction of gravity discontinuities already identified. We present below five interpreted seismic lines showing the main results obtained after the interpretation of the different seismic horizons.

Section S1 is oriented NW-SE (Fig. 1c); it is traced between the two blocks mentioned above in the gravimetric study which are separated by the N-S master fault noted F1 (Fig. 7). The mapping of the different horizons demonstrates that this fault has largely controlled sedimentation during the Lower Cretaceous period. Indeed, the SE block exhibits a reduced series of the sandy formations of Boudinar, Bouhedma and Sidi Aich, while they are thicker in the NW block. The NW end of the seismic section shows that the thickness of the Sidi Aich Formation increases considerably. Moreover, this extremity highlights a Triassic saliferous feature which is very well pronounced at depth. The NW block, characterizing the subsurface of Mhamla, Belkhir, Segui and Aoussaj, located between the fault F1 and the Triassic intumescence, shows that the deep architecture is dominated by a flat-bottomed syncline in which the clay, sandy, gypsum deposits of the Bouhedma Formation

occur. The SE block corresponds to the Fejij Plain in which the Bouhedma Formation outcrops with a much reduced thickness. Three main faults have been mapped on this seismic line and correspond to the so-called F1, F18 and F2 oriented respectively N-S, NE-SW and E-W defined in the gravimetric study.

Section S2 characterizes the NW block of the study area and is mainly oriented N-S (Fig. 1c). This section extends between the northern flank of the Jebel Oum Laagol anticline and the southern flank of the Jebel Belkhir anticline. From north to south, this section well highlights the F3 and F4 faults which are E-W oriented and the F17 (Fig. 8), called the Hadhifa fault, which constitutes a segment of the SAFC. Several thickness and facies variation are clear on this N-S oriented seismic section. Indeed, from south to north the Bouhedma Formation gradually decreases in thickness while the Sidi Aich Formation records a net increase in thickness. The Melloussi, Boudinar and Orbata formations keep a constant thickness along the seismic line (Fig. 8). Furthermore, two Triassic saliferous bulges characterize this seismic section, denoting intense halokinetic activity which appears to have started since the Barremian. This halokinetic activity coupled with the dynamics of faults F17 and F3 established a deep geometry materialized by two synclines separated by a narrow anticline.

Section S3 starts from the NW limb of the Zemlet Elbeidha anticline, crosses the Fejij Plain, then the Araguib Itama, Hajri, Menzel Habib plains and continues through Sabkhet

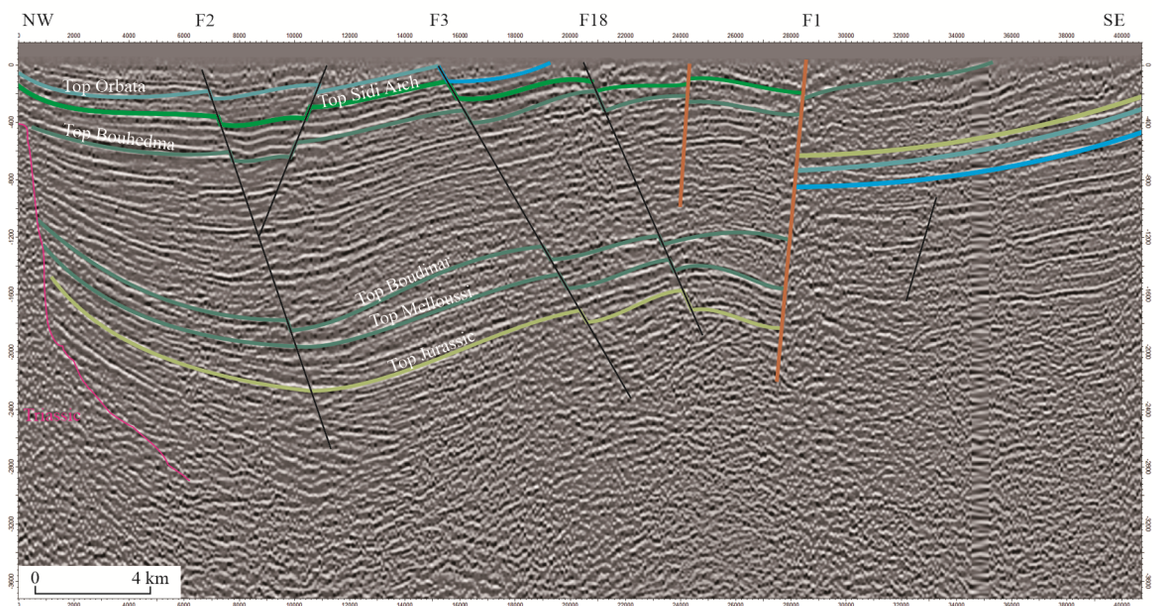

Figure 7. NW-SE interpreted seismic line showing the deep geometry of the MHP in response to the most major fault detected by gravimetric analysis. Note the role played by the F1 fault in the differentiation of two different basins, in the SE side, and the existence of Triassic intumescence, in the NW side.

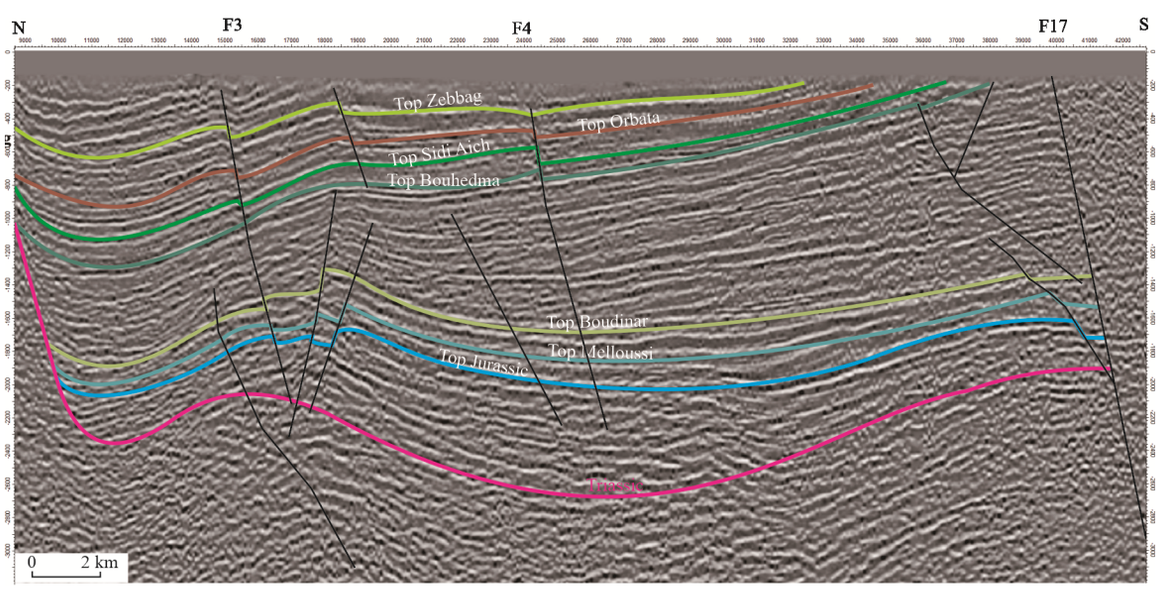

Figure 8. N-S interpreted seismic line showing the important role played by the F17 fault in the structuration of the subsoil of MHP and the thickening of the Early Cretaceous series in the northern side.

Sidi Mansour (Fig. 1c). It shows that the subsurface of these localities is compartmentalized, from south to north, into three distinct blocks bounded by four NE-SW, E-W and N-S oriented faults, corresponding respectively to F6, F8/F7 and F1 faults deduced from the gravimetric study (Fig. 9). These bordering faults of hidden basins have normal slip and show small reverse bends, which could be induced by progressive structural inversions. The latter, which occurred during the Maastrichtian-Eocene period and applying a maximum compressive stress in the NW-SE direction, has been widely demonstrated by Masrouhi et al. (2008) and Gharbi et al. (2015). it reactivates the NE-SW, E-W and N-S faults in reverse, reverse dextral and reverse sinister dynamics, respectively. In addition to these faults, this section shows the existence of two Triassic saliferous bulges delimiting a clear syncline depression. The structural-stratigraphic architecture presented by this section proves that these faults as well as the Triassic movement largely controlled sedimentation during the Lower Cretaceous. Indeed, south of the F7 fault, the Melloussi, Boudinar and Bouhedma formations show a strong reduction in thickness while the Sidi Aich Formation is at its maximum thickness. Gradually towards the north, the Bouhedma Formation gain in thickness with a small reduction above the salt structure evolving directly above the F1 fault while a depocentre is observed between the two salt structures for this formation. This architecture denotes that, during Early Cretaceous, sedimentation was contemporaneous with an active halokinetic rise.

Section 4 (Fig. 1c) with a NE-SW orientation, is orthogonal of Section 1 and crosses the subsurface of Zograta, Ouali and Aouled Khoud characterizing the NE province of the study area (Fig. 2). Several faults have been crossed by this section. From NE to SW, these faults correspond to the F12, F11, F13, F15, F16 and F9 previously detected by the gravimetric data (Fig. 10). Mapping of the different horizons shows that these faults have controlled sedimentation during Early Cretaceous. The central part, located between faults F15 and F16 shows that the Melloussi, Boudinar and Bouhedma formations declines dramatically in thickness while the Sidi Aich and Orbata formations are very thick. Towards the NE of fault F15 and to the SW of fault F9 the Sid Aich and Orbata formations become gradually thinner and the Melloussi, Boudinar and Bouhedma formations become thicker (Fig. 10). The deep architecture shown by this section is that of a large graben formed by the aforementioned faults showing a tectonic inversion of the ancient horst occurring from the Upper Barremian (Fig. 10).

Section 5 (Fig. 1c), with a E-W orientation, starts from Hajri and crosses the Sidi Mansour Sebkha, Mhamla, and Aoussaj plains. The different seismic horizons illustrated in this section makes it possible to clarify the role played by the F1 fault, oriented N-S, the F17 NW-SE oriented fault representing a segment of the SAFC and ends near a buried salt structure characterizing the subsurface of the plain of Bled Segui (Fig. 11). This seismic section shows that the deep structure crossed is compartmentalized into three blocks separated by the predicted faults. The compartment located east of the F1 fault shows that the Early Cretaceous formations are greatly reduced in thicknesses but the central block shows the thickest series. In addition, near the salt structure, these formations of the Lower Cretaceous become gradually thinner and show progressive pinchouts. This seismic section clearly proves that the sedimentation of the Lower Cretaceous is largely controlled by the normal play of the N-S and NW-SE faults and by the early halokinetic activity having probably started since Late Jurassic times (Zouaghi et al., 2007; Tanfous Amri et al., 2005), on the one hand, and that the sedimentary architecture induced is that of a mega tilted block towards the west, generated by the activity of the F1 fault, on the other hand (Fig. 11).

4.3 Facies and Thickness Variations

The Lower Cretaceous series are exposed only at Jebel Zemlet Elbeidha and Jebel Oum Laagol. The Melloussi and Boudinar formations as well as the lower part of the Bouhedma Formation are missing and do not outcrop. They are only seen in oil wells drilled in the region. To understand the role of the

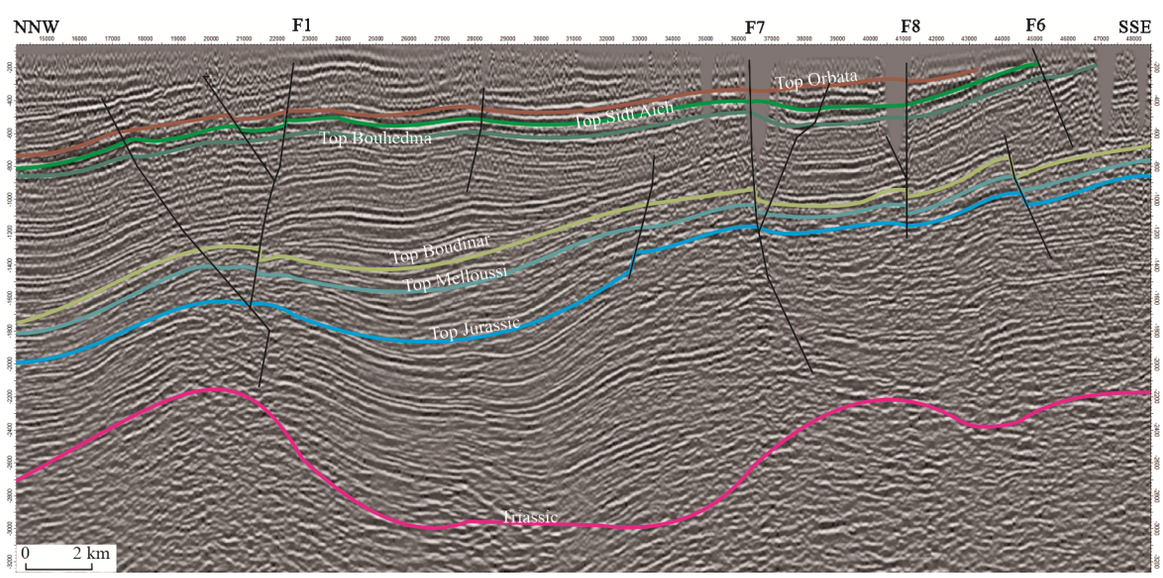

Figure 9. NNW-SSE interpreted seismic line presenting the tectonostratigraphic role accomplished by the F1 fault and the progressive thickening of the Early Cretaceous formations towards the NW.

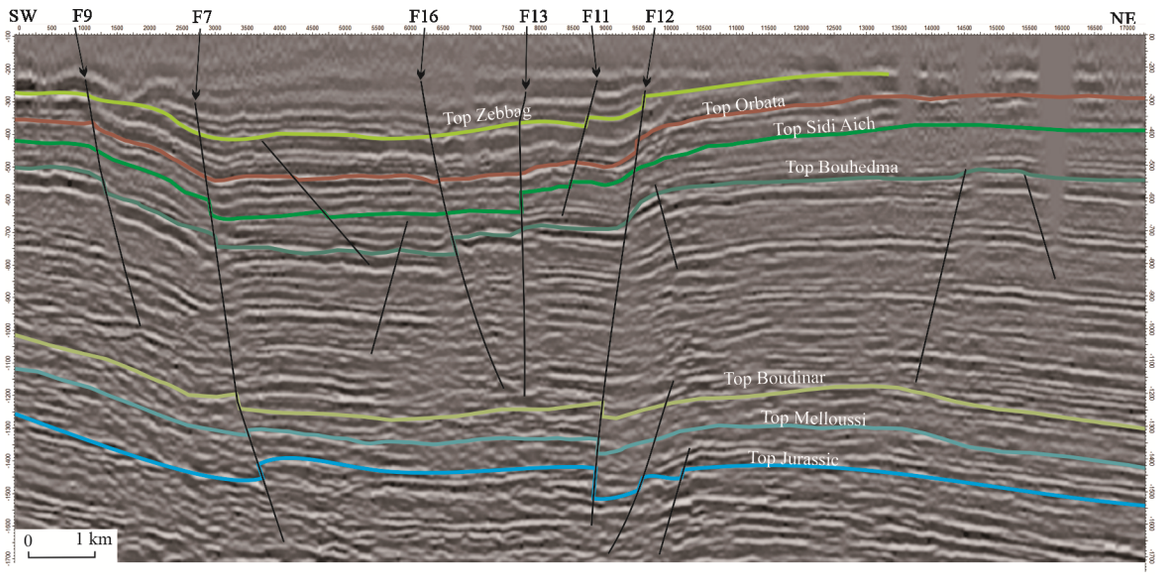

Figure 10. NE-SW interpreted seismic line demonstrating the general deep architecture of the eastern province.

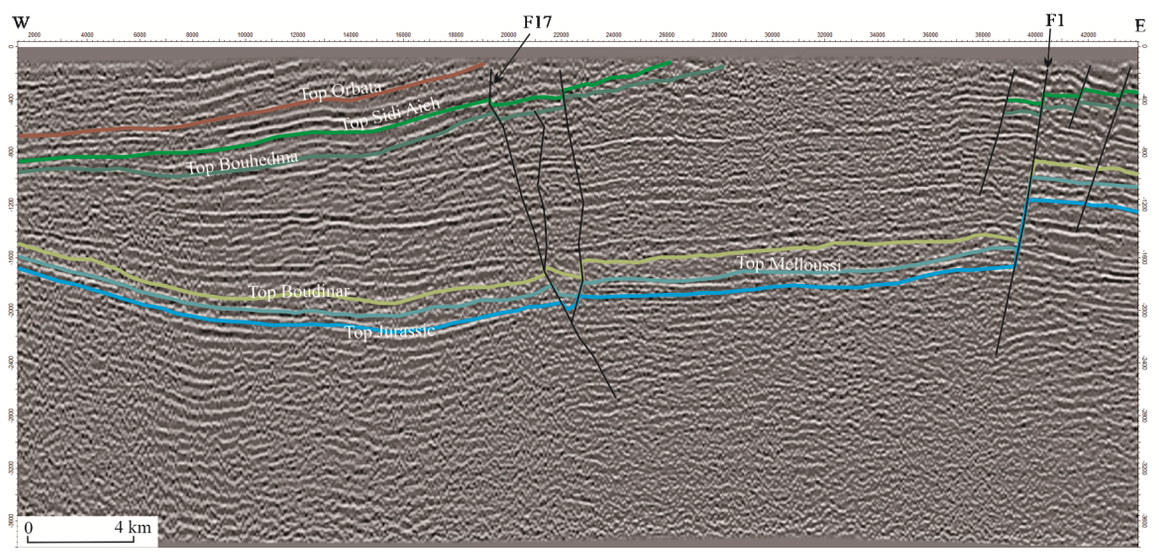

Figure 11. E-W interpreted seismic line crossing the MHP and showing the roles of the F1 and F17 faults in the structuration of the study area.

various faults in the distribution of these series, two correlation transect were carried out. The first one trends N-S (Fig. 12), using data from oil wells, while the second is oriented NE-SW (Fig. 13) highlighting the variations of facies and thicknesses of the outcropped series, at Jebel Zemlet Elbeidha, on both sides of the existing faults.

Figure 12 illustrates the first correlation line drawn in a N-S direction for the eastern part of the study area. From south to north, this correlation transect comprises four lithostratigraphic columns representative of the four petroleum wells ZB1, BHS1, BK1 and MAN1. The first two wells were drilled in the core of Zemlet Elbeidha anticline and at the centre of the MHP. Structurally, these two wells are separated by the F6 fault characterizing the NW flank of Zemlet Elbeidha. The BK1 well was drilled at the NE termination of Jebel Belkheir. These last two wells are separated by the layout of the N-S F1 fault. The MAN1 petroleum well characterizes the southern flank of Jebel Bouhedma.

Lithostratigraphic columns studied show significant facies and thicknesses variations of the different formations attributed to the Lower Cretaceous. Indeed, from south to north, we note a gradual thickness decrease of the Melloussi, Boudinar and lower part of the Bouhedma Formation. The lithostratigraphic column of the ZB1 petroleum well intersected a Bouhedma Formation three times thicker (1 300 m) than that crossed by MAN1 (420 m). The sandy part which characterizes the top of the Bouhedma Formation was encountered only at the ZB1 well with a thickness exceeding 150 m, while it is absent or greatly reduced in the other wells (30 m at BHS1). The thickness of the Melloussi and Boudinar formations is about 450 m in the Zemlet Elbeidha structure while it does not exceed 250 m in the Belkheir and Mansour structures.

In addition, a clear inversion of subsidence occurred during the Late Barremian-Aptian period. This inversion is shown by a strong thickness of the Sidi Aich and Orbata formations, in the north (Jebel Belkheir and Mansour 500 m), and a pro-

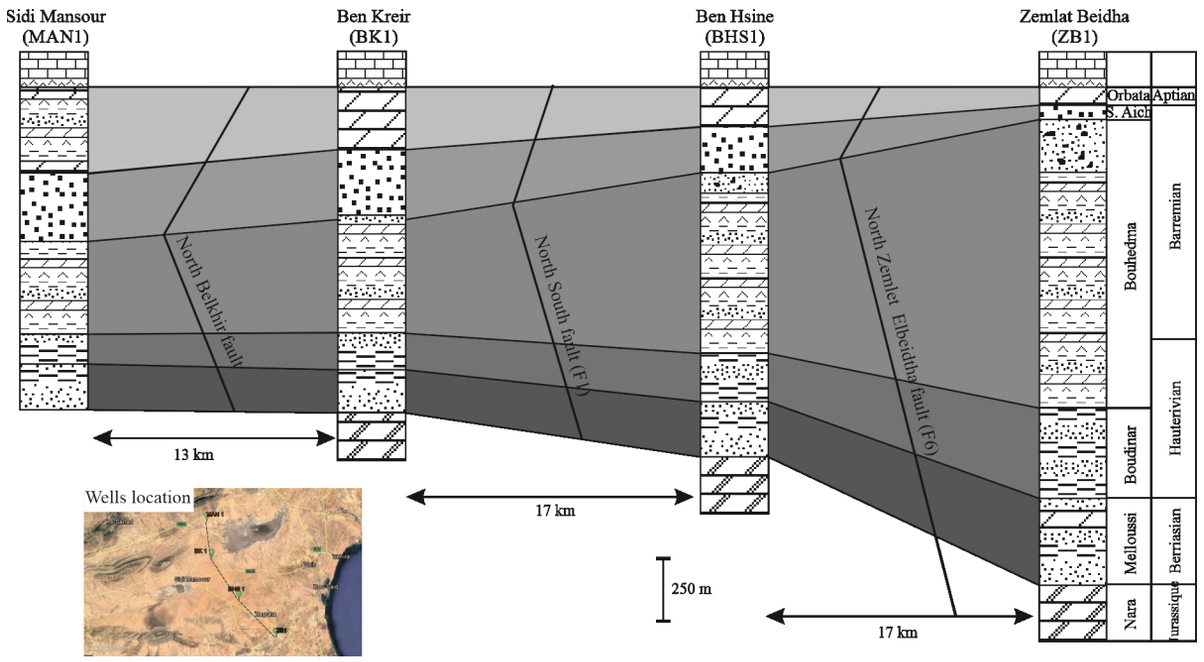

Figure 12. NNW-SSE correlation line of the Early Cretaceous formations crossed by the different oil wells characterizing the study area. Noting the clear change in fault dip that occurred from Late Barremian inducing a change in subsidence which becomes the NW oriented.

gressive reduction of this thickness towards the south (Zemlet Elbeidha structure) where it is at most 100 m thick. We also note that the Orbata Formation, drilled by the MAN1 petroleum well, is formed by clays and dolomites while it is exclusively dolomitic in the other localities.

Figure 13 illustrates the second correlation line which is mainly oriented NE-SW. It comprises six lithostratigraphic columns characterizing the southern limb of the Zemlet Elbeidha anticline (Fig. 13a). Each column is separated from another by a directional fault (Fig. 13a). Significant thickness and facies variations are highlighted by this correlation line. It shows that the sandy deposits, characterizing the summit part of the Bouhedma Formation, as well as the Sidi Aich sandy formation shows, at the L4 locality, the great thinning. On both sides of this locality these sandy formations recorded a progressive increase in their thickness (Fig. 13b). This sedimentary effect, during this period, is controlled by the normal activities of the different defined faults inducing a horst and graben architecture (Fig. 13c).

In addition, dolomites attributed to the Orbata Formation show continuous variations from one locality to another (Fig. 1b). The lithostratigraphic column L3 exposes the thinnest series and the column L5 demonstrates that the Orbata Formation is limited to two meters of conglomerates. The thickest series has been identified on column L4. This sedimentary effect is largely controlled by the normal activity of the various faults characterizing the southern side of the Zemlet Elbeidha structure which induces a horst and graben architecture (Fig. 13d) but conversely with the structuration of the underlying sandy series.

4.4 Synsedimentary Faulting Analysis

To determine the structural evolution of the NE termination of the southern Atlas including the MHP, during the Early Cretaceous, we measured the orientations of striations on fault planes affecting different formations. Syndepositional fault populations, providing direct dating of tectonic events, have been especially analysed. Deposits attributed to the Valanginian and the Hauterivian, defining the Melloussi and Boudinar formations, do not outcrop in our sector of study. For this reason, we focused on to the synsedimentary faults affecting the Bouhedma, Sidi Aich and Orbata formations which are exposed at Jebel Zemlet Elbeidha and Jebel Oum Laagol. We present below the main sites fossilizing tectonic events during the Early Cretaceous.

Red marly, and beige to yellow sand alternations, attributed to the Late Hauterivian period, outcrop at the core of Zemlet Elbeidha anticline, preserving many syndepositional normal faults. These last are organized into two directional sets (Fig. 14a). The first set contains N40°-N60° trending faults while the second one is represented by NW-SE oriented faults. These syndepositional faults impose a horst and graben design. The numerical treatment of these fractures shows that the Late Hauterivian sedimentation is controlled by extensive tectonics applying a N-S trending minimal horizontal stress (Figs. 14a' and 14b).

Several normal synsedimentary faults (Figs. 14c and 14d) affecting clay, dolomite and gypsum alternations, attributed to the Hauterivian and Barremian periods and defining the Bouhedma and Sidi Aich formations, characterize the Jebel Oum Laagol show that this sedimentation was controlled by an extensive tectonics involving a N-S trending minimum stress (Figs. 14c' and 14d').

The red dolomitic bar which marks the summit of the Bouhedma Formation, which outcrops between Khanguit Amor and Khanguit Aicha at the southern limb of Zemlet Elbeidha anticline, is affected by multitudes of normal synsedimentary faults (Fig. 14e). These are oriented E-W, NE-SW and

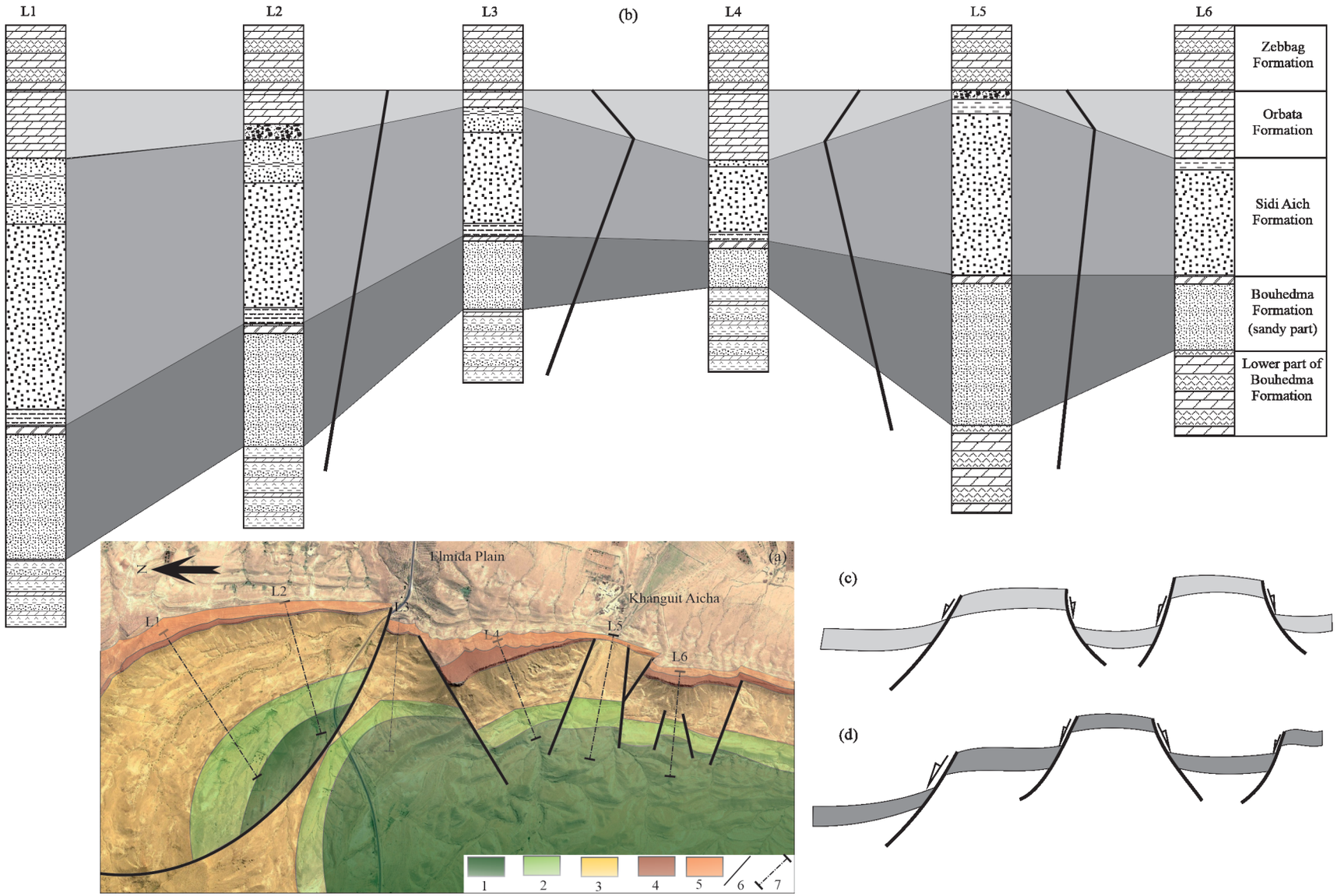

Figure 13. Role of the different network of faults affecting the southern flank of the Zemlet Elbeidha anticline in the distribution of the Barremian and Aptian sedimentation. (a) Simplified geological map of the southern flank of the Zemlet Elbeidha anticline showing the location of the different lithological columns correlated (1 and 2: middle and top parts of the Bouhedma Fm; 3: Sidi Aich Fm; 4: Orbata Fm; 5: Upper Cretaceous; 6: faults; 7: location of sections); (b) correlation line of the Barremian-Aptian formations characterizing this site; (c) and (d) fault geometries during sedimentation demonstrating a clear fault dipping change from Barremian to Aptian periods.

NW-SE and create an architecture of horsts and grabens. Numerical analyses of these fractures shows that the Late Barremian sedimentation is controlled by an extensive tectonic event applying a N-S to NNE-SSW trending minimal horizontal stress (Fig. 14e').

Dolomites attributed to the Aptian period, which characterise the Orbata Formation are affected by normal faults trended NE-SW, NW-SE and E-W (Figs. 14f, 14g and 14h). These faults create a tilted blocks and a horst and graben geometries (Fig. 14h). Numerical analyses of these faults prove that the Aptian sedimentation was subjected to an extensive tectonic regime applying a NE-SW minimal stress (Figs. 14f', 14g', 14h' and 14i).

5 DISCUSSION: PALEOSTRUCTURATION

The multiscale approach adopted to understand the geodynamic evolution of the MPH, based on the morphological analysis and the interpretation of gravity and seismic data coupled with the inventory of facies and thickness variations of the Lower Cretaceous Formations and the examination of the syn-sedimentary faults proves that this plain was dominated, during the Early Cretaceous time, by N-S to NE-SW extensive forces. This tectonic event resulted in the creation of separate individual basins, of variable sizes and extents, evolving due to a complex network of faults.

Morphological analysis allows us to note that the MHP is differentiated, from east to west, into two different hydrological provinces separated by a N-S oriented topographic bulge which is traced in the center of this plain and serves as a water shed (Fig. 3). It corresponds to a surface response of a deep fault (Figs. 6 and 9) elongated in the same direction. Regionally, this morphologic high constitutes the extension towards the south of the morphostructural line, elongated from Hammem Lif, in the north, to Mezzouna, in the south, which is formed on a N-S paleogeographic fault, commonly called the N-S Axis. Although, morphologically not very prominent, this sub-central uplift reflects the effects of an irregular geodynamic evolution and plays a very important role in the structural differentiation of the Menzel Habib Basin.

The most impressive gravimetric differentiation is that shown by an N-S trending fault separating an eastern basin (with the signature of a dense rock series) and a western basin characterized by a significant mass deficit (Fig. 5a). This fault coincides with one identified by morphological analysis and corresponds to the southernmost branch of the N-S Axis. The residual map, the vertical and horizontal gradient maps as well as the tilt angle map show that the subsurface of MHP is shaped into several E-W and NE-SW trending basins which are largely disturbed by N-S, NE-SW, E-W and NW-SE oriented faults (Fig. 6b).

The interpretation of the available seismic lines confirmed the existence of the whole faults detected by the morphological and gravimetric analysis. These faults determine the distribution of the various geological formations that characterize the study area during basinal stage evolution and guided its structural differentiation during the Late Cretaceous tectonic inversion which apply a NW-SE compressive stress. This tectonic inversion has resulted in the final installation of the current structures which are represented by folds, diapirs and various faults that characterize the region. The most important salt structures are located below faults F1, F17 and F8 which characterize the subsurface of Menzel Habib Village-Jebel Belkheir, the north flank of Jebel Oum Laagol and the subsurface of Sabkhet Sidi Mansour-Mhamla, respectively. The Triassic outcrop of Jebel Hadhifa constitutes the ultimate vertical diapiric evolution of the Triassic salt through the F17 fault resulted from the successive tectonic compressions of the Upper Cretaceous and the Tertiary periods.

The F1 and F17 faults, which present a N-S and NW-SE direction respectively, are the most important faults that have contributed to the shaping of the study area. In addition, the geodynamic evolution of the region is also due to the E-W and NE-SW faults, currently exhibiting reverse and sinistral reverse activities respectively.

During the Early Cretaceous period, the extensive dynamics governing the Tunisian margin and applying a N-S to NE-SW minimal stress, activates the F1 fault with a normal dynamic allowing the uplift of the eastern block and the subsidence of the western one (Fig. 15). This architecture promotes accumulation of a thick and continues series to the west and a reduced thickness in the eastern province (Fig. 4a). During the Lower Barremian, the sandy deposits of the Bouhedma Formation seal the various faults and fill the various blocks and provinces mentioned above. From the Upper Barremian, following the change in the direction of the minimum stress which becomes oriented NE-SW, the NW-SE (F17) and E-W faults (F3, F4 and the Jebel Chamsi-Belkheir fault) change their dip and become dipping towards the north favoring a progressive thickening of the Sidi Aich and Orbata formations from the south to the north. This sedimentation defines a tilted block architecture. At the same time, following an E-W transect, the N-S faults (F1 and its parallel) delimit a high zone corresponding to the eastern province of the study area which is bordered on both sides by two grabens recording strong sedimentation (Fig. 15).

From north to south, Burollet (1956), Abbès et al. (1981), Boccaletti et al. (1988), Doglioni et al. (1990), Martinez et al. (1991) and Arfaoui et al. (2015) demonstrated that this architecture has been proven on all the different branches of the N-S Axis. Furthermore, this master lineament constitutes a sedimentary limit between two domains, which have different paleogeographic settings, the Atlas zone, with very thick Lower Cretaceous formations, and the eastern platform, characterizing a slow subsidence. Arfaoui et al. (2015) denoted that this alignment has formed a paleogeographic feature since the Jurassic as the reductions or condensations of the sedimentary sequences often show gaps and unconformities.

In addition, in response to this extensive feature, the F17 fault, representing the south-easternmost branch of the SAFC, was activated as normal fault dipping to the north-east (Fig. 15). It resulted in an accumulation of a continuous and thick series in the northest part (3 000 m thick of deposits) and reduced ones in the SW province in which the total thickness of the Jurassic and Early Cretaceous series does not exceed 1 600 m (Hlaiem, 1999). This architecture has been highlighted and proven by Saïd et al. (2011) and Arfaoui et al. (2015). These two authors have confirmed that these major faults were

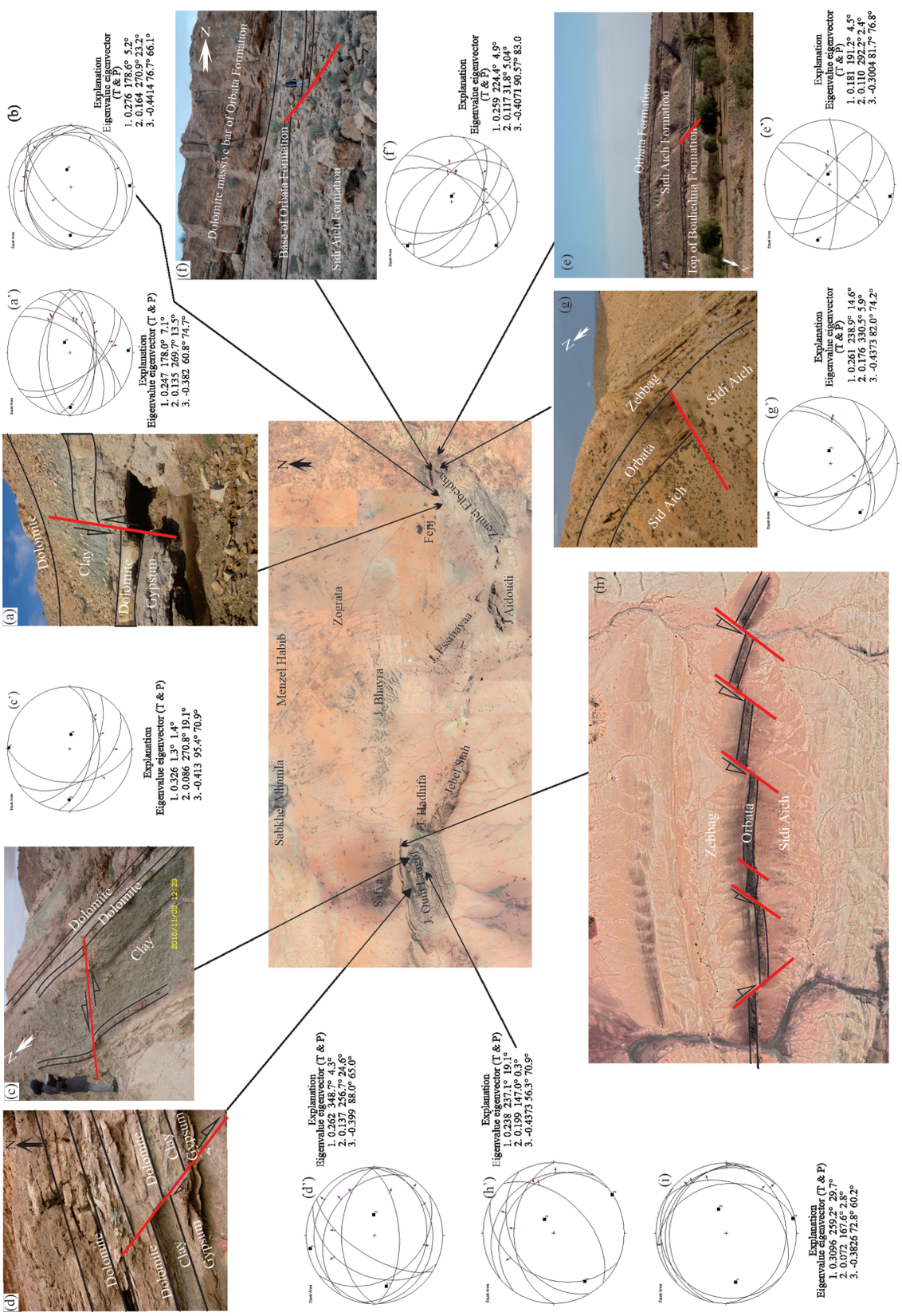

Figure 14. Syndepositional faulting affecting the Barremian-Aptian deposits recorded at the different outcropped series in the study area (a), (c), (d), (e), (f), (g) and (h) and characteristic stereographic projections corresponding to data measurements, Schmidt projection, lower hemisphere (b), (a'), (c'), (d'), (e'), (f'), (g'), (h') and (i) (the central figure shows the location of the studied sites); fault planes are great circles; slickenside lineations are small centrifugal arrows (normal faults); black squares with index 1, $\sigma 3$; black squares with index 2, $\sigma 2$; black squares with index 3, $\sigma 1$.

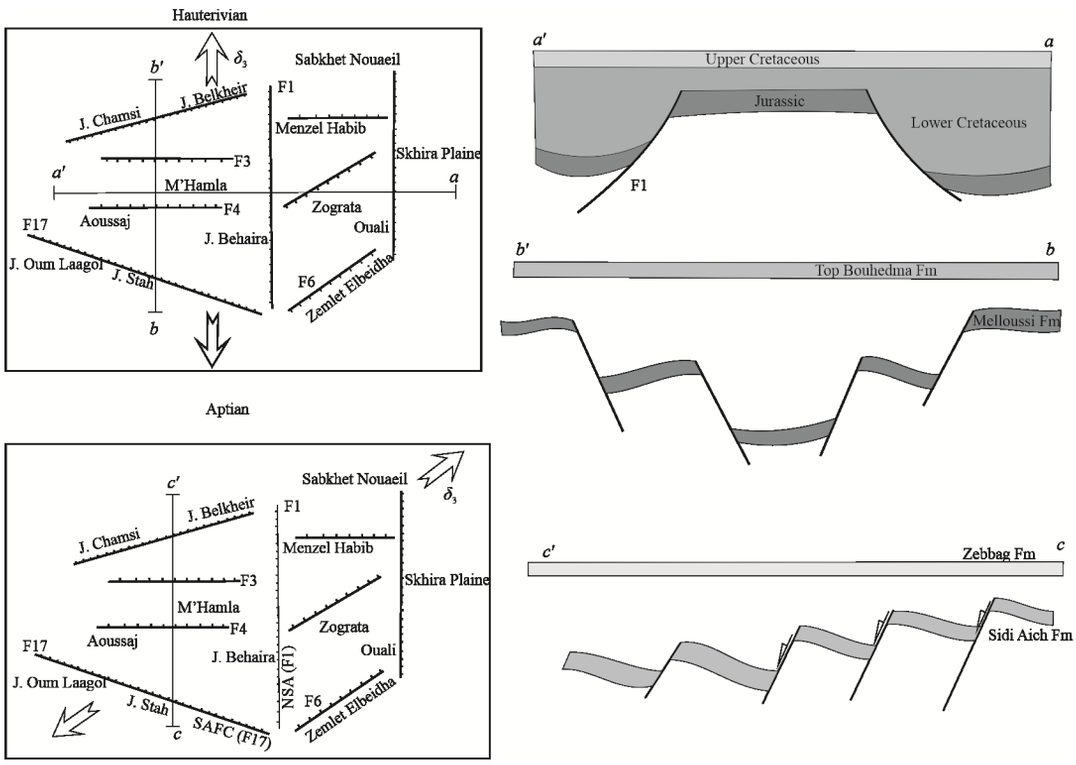

Figure 15. Two evolutionary models of Menzel Habib Plain in relation to the most important fault which affects the study area and in response to the N-S and NE-SW extensional tectonics.

caused by, during the Late Triassic to Early Cretaceous, the initiation and the accommodation of the Tethyan rifting and induced a complex system of horst and graben structures.

Both the N-S Axis faults and the Gafsa-Hadhifa accident lead us to consider them as first order structures to which the MHP owes its existence and its evolution since the first stages of Tethyan rifting.

Second, the stratigraphic evolution of the MHP depends on the NE-SW fault, which runs along the NW flank of Zemlet Elbeidha, and the E-W fault which borders Jebel Belkheir and Jebel Chamsi on the south. During the Valanginian-Hauterivian these two faults dip towards the south while they dip towards the north during the Barremian to Aptian period (Fig. 15).

In response to the Early Cretaceous NE-SW to N-S extensive tectonics, these faults compartmentalized the subsurface of Sidi Mansour-Mhamla-Aoussaj into several rhombic basins of different geometries and sizes with differential migration of the subsidence. This architecture is that of a large graben made by the Hadhifa fault (F17) which dips toward the north and the major E-W fault bordering the Jebel Chamsi and Jebel Belkheir anticline's, and which dips to the south (Fig. 15). On the other hand, the F1 fault and the major fault separating the MHP from the Plain of Skhira which plunge towards the west and towards the east respectively, delimit a great horst characterizing the subsurface of Zograta-Rbiat Ouali (Fig. 15).

Detailed analysis of the different syndepositional faults preserved in the Early Cretaceous series proves that this extensive tectonic event applied two successive minimum stress events oscillating between N-S and NE-SW poles. The first direction of stress is attributed to the Valanginian-Barremian period while the second one characterizes the Late Barremian to Aptian time.

In addition to their synsedimentary activity these faults guided, during the Lower Cretaceous, significant halokinetic activity which is observed as Triassic pillows and diapirs. Some of these Triassic salt diapirs reach the surface, such as at Jebel Hadhifa (Fig. 1), others remain buried and mark out the layout of the major faults, for example the case of the Triassic pillow on the F1 fault (Figs. 8 and 9). These salt bodies implanted on the master faults give an additional argument on the role played by these faults in the geodynamic evolution of the MHP. Chronologically, the N-S extensional tectonics recorded at this region of the Tunisian margin started in the Triassic period. It has been highlighted at the south-eastern part of Tunisia (Raulin et al., 2011; Bouaziz et al., 2002) in the central Tunisian Atlas (Soussi, 2000; Martinez et al., 1991; Soyer and Tricart, 1987) and in the northern Tunisian Atlas (Ben Chelbi et al., 2008; Boughdiri et al., 2006; Morgan et al., 1998). This extensional event evolved in relation with the sub-meridian Tethyan extensional framework, which affected the whole of the North-African margin (Zouaghi et al., 2011).

This extensive event, which controlled the Tunisian margin during the Lower Cretaceous, has been widely studied and proven in Libya (Jolivet et al., 2016; Abadi et al., 2008; Coward and Ries, 2003), in Italy (Chirchi and Trémolière, 1984) in Algeria (Yelles-Chaouche et al., 2001; Guiraud and Bellion, 1995; Guiraud and Maurin, 1991), in Morocco (Ait Brahim et al., 2002; Piqué et al., 1998), and in Spain (Platt et al., 2013; Comas et al., 1999). It is responsible for an intense rifting applying N-S and NE-SW faults favoring the development of sev-

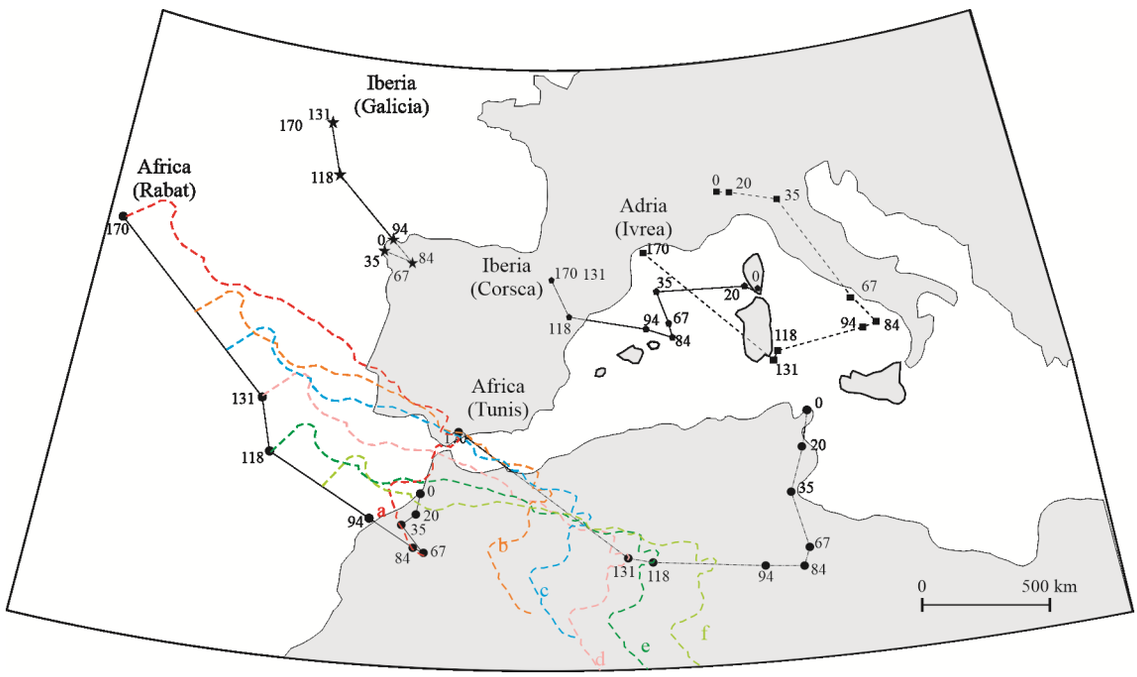

Figure 16. Relative motion of Africa with respect to Europe. Six steps (a, b, c, d, e and f with different colors) of displacement of Tunis summarize the relative trajectory of Africa during Early Cretaceous (Handy et al., 2010).

eral NE-SW trending grabens filled with continental deposits. Moreover, this distension is accompanied by very important basaltic magmatism (Laridhi Ouazaa et al., 2004).

The extensive tectonics which controls the Tunisian margin as well as the neighboring margins and which applies two minimal stress directions, trended NS and NE-SW, representative of the Valanginian-Hauterivian-Lower Barremian and the Upper Barremian-Aptian times respectively, translate the echoes of a the irregular evolutionary motion of Africa and Iberia in respect to the Eurasian plates during Tethyan and Atlantic spreading (Fig. 16) (Handy et al., 2010; Capitanio and Goes, 2006; Rosenbaum et al., 2002). The first geodynamic stage of extension is contemporaneous to the northward propagation of the Atlantic Ocean spreading along the western margin of Iberia and the sinistral displacement of Africa relative to Europe (Figs. 16 and 17) (Stampfli and Borel, 2002; Dercourt et al., 1985) which produced the abandonment of the Ligurian-Tethys corridor and the opening of the Bay of Biscay along the already rifted Pyrenean Basin with a concurrent counter clockwise rotation of Iberia (Vissers and Meijer, 2012; Handy et al., 2010; Gong et al., 2008). The second geodynamic stage characterized by NE-SW dynamics results from the northward propagation of the Central to North Atlantic which led to the separation and eastward motion of the Iberian microplate and Africa with respect to Europe (Figs. 16 and 17b) (Guerrera et al., 2021; Ye et al., 2017; Menant et al., 2016; Berra and Angiolini, 2014; Handy et al., 2010). After this significant plate reorganization and increase of the Iberia-Africa-Eurasia convergence velocity at ~118 Ma (Jolivet et al., 2016; Agard et al., 2007), it resulted in the onset of subduction of the eastern Ligurian part of Alpine Tethys along the Iberian-African plate boundary which was continuous with intracontinental subduction and Eo-Alpine orogenesis (Fig. 17b) at the northern tip of Adria, where Alcapia and Adria converged obliquely during the same time period (Ye et al., 2017; Jolivet et al., 2016; Handy et al., 2010).

In our case, the change of stress field from a N-S pole to a NE-SW one represents the transition between the opening of the South Atlantic, the sinistral drift towards the SE of Africa in relation to Eurasia and the beginning of subduction of the Neo-Tethys (Lustrino and Wilson, 2007; Carminati and Doglioni, 2005; Rosenbaum et al., 2002; Doglioni et al., 1999), and the beginning of the opening of the eastern Mediterranean accompanied by the NW migration of Apulia and the development of back-arc basins above the northern subduction zone, forming the oceanic crust now flooring the Black Sea and the Caspian Sea (Jolivet et al., 2016; Nikishin et al., 2015a, b, 1998; Agard et al., 2014; Hippolyte et al., 2010).

6 CONCLUSIONS

The main results on structural-stratigraphic field investigations and the analysis of gravimetric and seismic data, targeting at the Menzel Habib Plain, which represents a hinge zone between the major structural features of the southern Tunisian margin, can be summarized as follows.

(a) The hydrographic and morphologic approach proves that the MHP is subdivided into two distinguishing hydrologic basins separated by a N-S topographic high which express the surface response of the deep activity of a N-S trending fault (F1) constituting the southward continuity of the called N-S Axis.

(b) The synsedimentary faults affecting the various formations of the Early Cretaceous as well as the variations in thickness and facies of these formations, on both sides of the major faults, prove that this period was controlled by an extensive tectonic events applying a minimal stress that oscillated between a N-S pole and a NE-SW pole. The Valanginian-Hauterivian-Lower Barremian period, with a N-S extensive event, consti-

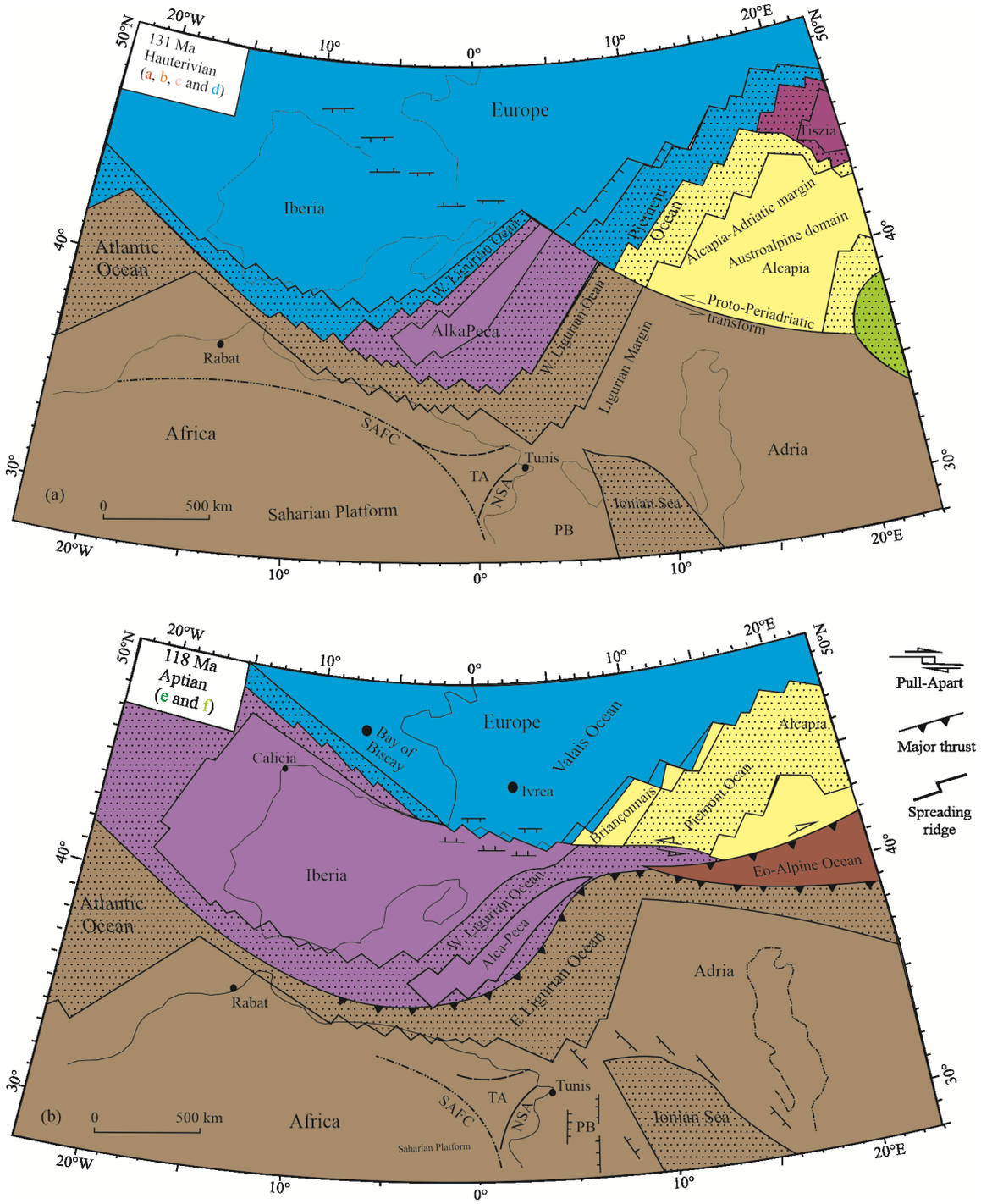

Figure 17. Plate tectonic maps of Alpine Tethys and the western embayment of Neotethys during Hauterivian and Aptian periods, respectively (Handy et al., 2010). SAF. South Atlasic fault; TA. Tunisian Atlas; NSA. North South Axis; PB. Pelagean Block; SP. Saharian Platform; SAFC. South Atlasic fault corridor.

tutes the continuation of the long rifting epoch, which began in the Late Triassic time and which is responsible for the creation of several basins evolving in respect to N-S and NW-SE normal faults. From the Late Barremian period, the minimum stress became NE-SW. It is responsible for the amplification of the subsidence of the basins following a horst and graben or tilted block architecture. The N-S, E-W and NW-SE faults are the most important and the most imposing syndepositional faults to ensure this evolution.

(c) Lower Cretaceous sedimentation was largely guided by irregular activities recorded on the N-S, NW-SE and E-W faults, respectively describing the F1 fault, the F17 fault and the fault bordering Jebel Chamsi on the south side. In response to the extensive tectonic events of this period, these faults show respective dips to the west, to the NE and to the south, thus delimiting a depocenter characterizing the western province of the study area. This architecture promotes accumulation of a thick and continuous series to the west and a reduced thick-

ness in the eastern province.

(d) The deep architecture of the MHP, deduced from the available gravity maps, is that of two basins with rocks of different densities, separated by a major N-S oriented fault (F1). In response to the extensive events, characterizing the Early Cretaceous period, this faults have acted as a normal fault dipping to the west and causing the collapse of the western province and the rise of the eastern one. The eastern compartment is formed by a thin and dense series while the western basin is characterized by a significant mass deficit. The residual map, the vertical and horizontal gradient maps as well as the tilt angle map show that the subsurface of the MHP is formed into several E-W and NE-SW trending basins which are largely cut by N-S, NE-SW, E-W and NW-SE oriented faults.

(e) The available seismic lines clearly confirmed the existence of all the faults detected by the gravimetric and morphologic analysis. The most important faults highlighted by the seismic interpreted lines are the F17 fault, representing the most eastern branch of the SACF, and the F1 fault which constitutes the southern segment of the NSA.

These results prove that the MHP recorded, during the Lower Cretaceous, an extensive geodynamic evolution similar to that described in the rest of the Tunisian margin which was initiated since the Jurassic. This dynamic is responsible for the development of sedimentary basins of various sizes and shapes in relation to the different fault systems on which they evolve. Moreover, the MHP records a basin evolution strictly guided by the repeated activities of the major faults of the southern margin of Tunisia (the SACF and the NSA). This evolution represents the echoes of the sliding movements of Africa in relation to Europe and the beginning of the opening of the Pelagean Sea.

ACKNOWLEDGMENTS

The author is grateful to James Bleach and Rob Wallace from the ōbex project for language editing support. The author would like to express thanks and gratitudes to the editors and the anonymous reviewers for their constructive comments which improved this article. The final publication is available at Springer via https://doi.org/10.1007/s12583-021-1540-x.

REFERENCES CITED

Abadi, A. M., van Wees, J. D., van Dijk, P. M., et al., 2008. Tectonics and Subsidence Evolution of the Sirt Basin, Libya. *AAPG Bulletin*, 92(8): 993–1027. https://doi.org/10.1306/03310806070

Abbès, C., Turki, M. M., Truillet, R., 1981. Un Elément Structural Nouveau dans L'Atlas Tunisien: le Contact Tangentiel Décakilometrique à Vergence Ouest des Djebels Ousselat et Bou Dabous (Axe Nord-Sud-Tunisie). *Comptes Rendus Académie Sciences*, *Paris*, 292(II): 473–476

Agard, P., Jolivet, L., Vrielynck, B., et al., 2007. Plate Acceleration: The Obduction Trigger? *Earth and Planetary Science Letters*, 258(3/4): 428–441. https://doi.org/10.1016/j.epsl.2007.04.002

Agard, P., Zuo, X., Funiciello, F., et al., 2014. Obduction: Why, how and where. Clues from Analog Models. *Earth and Planetary Science Letters*, 393: 132–145. https://doi.org/10.1016/j.epsl.2014.02.021

Ait Brahim, L., Chotin, P., Hinaj, S., et al., 2002. Paleostress Evolution in the Moroccan African Margin from Triassic to Present. *Tectonophysics*, 357(1/2/3/4): 187–205. https://doi.org/10.1016/s0040-1951(02)00368-2

Arfaoui, M., Reid, A., Inoubli, M. H., 2015. Evidence for a New Regional NW-SE Fault and Crustal Structure in Tunisia Derived from Gravity Data. *Geophysical Prospecting*, 63(5): 1272 – 1283. https://doi. org/10.1111/1365-2478.12248

Ben Chelbi, M., 2019. La Compression de L'Albo-Cenomanien dans la Marge Tunisienne Preuve Géostructurale de la Phase Autrichienne et Prémices de L'inversion Tectonique. 2ème Colloque International sur la Géologie de la Chaîne des Maghrébides et des Régions Voisines. Sétif, al Gérie du 4 AU 6 Décembre 2018

Ben Chelbi, M., 2021. Geodynamic Evolution of the Tunisian Margin during the Albian-Cenomanian: Structural Evidence of the Austrian Orogenic Phase and the Early Tectonic Inversion of the Tunisian Atlas. *Journal of the Geological Society*, 178(3). https://doi. org/10.1144/jgs2019-195

Ben Chelbi, M., Kamel, S., Harrab, S., et al., 2013. Tectonosedimentary Evidence in the Tunisian Atlas, Bou Arada Trough: Insights for the Geodynamic Evolution and Africa-Eurasia Plate Convergence. *Journal of the Geological Society*, 170(3): 435 – 449. https://doi. org/10.1144/jgs2012-095

Ben Chelbi, M., Melki, F., Zargouni, F., 2006. Mode de Mise En Place des Corps Salifères Dans L'Atlas Septentrional de Tunisie. Exemple de L'appareil de Bir Afou. *Comptes Rendus Geoscience*, 338(5): 349 – 358. https://doi.org/10.1016/j.crte.2006.02.009

Ben Chelbi, M., Melki, F., Zargouni, F., 2008. Précision sur L' évolution Structurale de L'Atlas Septentrional de Tunisie Depuis le Crétacé (Bassin de Bir M'Cherga). Echos d'une Evolution Polyphasée de la Marge Tunisienne Dans Son Cadre Méditerranéen. *Africa Geosciences Review*, 15(3): 229–246

Berra, F., Angiolini, L., 2014. The Evolution of the Tethys Region Throughout the Phanerozoic: A Brief Tectonic Reconstruction. *AAPG Memoir*, 106: 1–27. https://doi.org/10.1306/13431840m1063606

Boccaletti, M., Cello, G., Tortorici, L., 1988. Structure and Tectonic Significance of the North South Axis of Tunsia. *Annales Tectonicae*, 1(II): 12–22

Bodin, S., Petitpierre, L., Wood, J., et al., 2010. Timing of Early to Mid-Cretaceous Tectonic Phases along North Africa: New Insights from the Jeffara Escarpment (Libya-Tunisia). *Journal of African Earth Sciences*, 58(3): 489–506. https://doi.org/10.1016/j.jafrearsci.2010.04.010

Bouaziz, S., Barrier, E., Soussi, M., et al., 2002. Tectonic Evolution of the Northern African Margin in Tunisia from Paleostress Data and Sedimentary Record. *Tectonophysics*, 357(1/2/3/4): 227 – 253. https://doi.org/10.1016/s0040-1951(02)00370-0

Boughdiri, M., Sallouhi, H., Maâlaoui, K., et al., 2006. Calpionellid Zonation of the Jurassic-Cretaceous Transition in North-Atlasic Tunisia. Updated Upper Jurassic Stratigraphy of the 'Tunisian Trough' and Regional Correlations. *Comptes Rendus Geoscience*, 338(16): 1250–1259. https://doi.org/10.1016/j.crte.2006.09.015

Burollet, P. F., 1956. Contribution à L' étude Stratigraphique de La Tunisie Centrale. Annales Mines et Géololgie, Tunis. 18: 350

Capitanio, F. A., Goes, S., 2006. Mesozoic Spreading Kinematics: Consequences for Cenozoic Central and Western Mediterranean Subduction. *Geophysical Journal International*, 165(3): 804 – 816. https://doi.org/10.1111/j.1365-246x.2006.02892.x

Carminati, E., Doglioni, C., 2005. Europe: Mediterranean Tectonics. Encyclopedia of Geology. Elsevier, Amsterdam. 135 – 146. https://doi.org/10.1016/b0-12-369396-9/00135-0

Chirchi, A., Trémolière, P., 1984. Nouvelles Données sur L' évolution Structurale au Mésozoïque et au Cénozoïque de la Sardaigne et leurs Implications Géodynamiques dans le Cadre Méditerranéen. *Comptes*

Rendus Académie Sciences Paris, 298(20): 889–894

Comas, M. C., Platt, J. P., Soto, J. I., et al., 1999. The Origin and Tectonic History of the Alboran Basin: Insights from Leg 161 Results. *Proceedings of the Ocean Drilling Program Scientific Results*, 161: 555–580. https://doi.org/10.2973/odp.proc.sr.161.262.1999

Coward, M. P., Ries, A. C., 2003. Tectonic Development of North African Basins. *Geological Society*, *London*, *Special Publications*, 207(1): 61–83. https://doi.org/10.1144/gsl.sp.2003.207.4

Dercourt, J., Zonenshain, L. P., Ricou, L. E., et al., 1985. Présentation de 9 Cartes Paléogéographiques au 1/20 000 000 s'étendant de L'Atlantique au Pamir Pour la Période du Lias à L'Actuel. *Bulletin Société Géologique France*, 8(I5): 637–652

Doglioni, C., Bosellini, A., Frare, M. C., et al., 1990. Annali Dell Universita di Ferrara. *Scienze della Terra*, 2(5): 77–94

Doglioni, C., Gueguen, E., Harabaglia, P., et al., 1999. On the Origin of West-Directed Subduction Zones and Applications to the Western Mediterranean. *Geological Society*, *London*, *Special Publications*, 156(1): 541–561. https://doi.org/10.1144/gsl.sp.1999.156.01.24

Doglioni, C., Mongelli, F., Pieri, P., 1994. The Puglia Uplift (SE Italy): An Anomaly in the Foreland of the Apenninic Subduction Due to Buckling of a Thick Continental Lithosphere. *Tectonics*, 13(5): 1309–1321. https://doi.org/10.1029/94tc01501

Ghanmi, M., Bahrouni, A., Ghanmi, M., et al., 2017. Aptian-Albian Boundary in Central Southern Atlas of Tunisia: New Tectono-Sedimentary Facts. *Journal of African Earth Sciences*, 132: 27 – 36. https://doi.org/10.1016/j.jafrearsci.2017.04.030

Gharbi, M., Masrouhi, A., Espurt, N., et al., 2013. New Tectono-Sedimentary Evidences for Aptian to Santonian Extension of the Cretaceous Rifting in the Northern Chotts Range (Southern Tunisia). *Journal of African Earth Sciences*, 79: 58–73. https://doi.org/10.1016/j.jafrearsci.2012.09.017

Ghedhoui, R., Deffontaines, B., Rabia, M. C., 2016. Neotectonics of Coastal Jeffara (Southern Tunisia): State of the Art. *Tectonophysics*, 676: 211–228. https://doi.org/10.1016/j.tecto.2015.11.032

Gong, Z., Langereis, C. G., Mullender, T. A. T., 2008. The Rotation of Iberia during the Aptian and the Opening of the Bay of Biscay. *Earth and Planetary Science Letters*, 273(1/2): 80 – 93. https://doi. org/10.1016/j.epsl.2008.06.016

Guerrera, F., Martín-Martín, M., Tramontana, M., 2021. Evolutionary Geological Models of the Central-Western Peri-Mediterranean Chains: A Review. *International Geology Review*, 63(1): 65–86. https://doi.org/10.1080/00206814.2019.1706056

Guiraud, R., Bellion, Y., 1995. Late Carboniferous to Recent, Geodynamic Evolution of the West Gondwanian, Cratonic, Tethyan Margins. The Tethys Ocean. Springer US, Boston, MA. 101 – 124. https://doi. org/10.1007/978-1-4899-1558-0_3

Guiraud, R., Bosworth, W., Thierry, J., et al., 2005. Phanerozoic Geological Evolution of Northern and Central Africa: An Overview. *Journal of African Earth Sciences*, 43(1/2/3): 83 – 143. https://doi. org/10.1016/j.jafrearsci.2005.07.017

Guiraud, R., Maurin, J. C., 1991. Le Rifting en Afrique au Cretace Inferieur; Synthese Structurale, Mise en Evidence de Deux Etapes Dans la Genese des Bassins, Relations Avec Les Ouvertures Oceaniques Peri-Africaines. *Bulletin de la Société Géologique de France*, 162(5): 811–823. https://doi.org/10.2113/gssgfbull.162.5.811

Handy, M. R., Schmid, S. M., Bousquet, R., et al., 2010. Reconciling Plate-Tectonic Reconstructions of Alpine Tethys with the Geological-Geophysical Record of Spreading and Subduction in the Alps. *Earth-Science Reviews*, 102(3/4): 121 – 158. https://doi. org/10.1016/j.earscirev.2010.06.002

Hippolyte, J. C., Müller, C., Kaymakci, N., et al., 2010. Dating of the Black Sea Basin: New Nannoplankton Ages from Its Inverted Margin in the Central Pontides (Turkey). *Geological Society*, *London*, *Special Publications*, 340(1): 113–136. https://doi.org/10.1144/sp340.7

Hlaiem, A., 1999. Halokinesis and Structural Evolution of the Major Features in Eastern and Southern Tunisian Atlas. *Tectonophysics*, 306(1): 79–95. https://doi.org/10.1016/s0040-1951(99)00045-1

Jolivet, L., Faccenna, C., Agard, P., et al., 2016. Neo-Tethys Geodynamics and Mantle Convection: From Extension to Compression in Africa and a Conceptual Model for Obduction. *Canadian Journal of Earth Sciences*, 53(11): 1190–1204. https://doi.org/10.1139/cjes-2015-0118

Khomsi, S., Bédir, M., Soussi, M., et al., 2006. Mise en Évidence en Subsurface D' événements Compressifs Éocène Moyen-Supérieur en Tunisie Orientale (Sahel): Généralité de la Phase Atlasique en Afrique du Nord. *Comptes Rendus Geoscience*, 338(1/2): 41 – 49. https://doi.org/10.1016/j.crte.2005.11.001

Lustrino, M., Wilson, M., 2007. The Circum-Mediterranean Anorogenic Cenozoic Igneous Province. *Earth-Science Reviews*, 81(1/2): 1 – 65. https://doi.org/10.1016/j.earscirev.2006.09.002

M'Rabet, A., Mejri, F., Burollet, P. F., et al., 1995. Catalog of Type Sections in Tunisia. *Cetaceous Memories ETAP*, 8A: 123

Martinez, C., Chikhaoui, M., Truillet, R., et al., 1991. Le Contexte Géodynamique de la Distension Albo-Aptienne en Tunisie Septentrionale et Centrale: Structuration Éocrétacée de L'Atlas Tunisien. *Eclogae Geologicae Helvetiae*, 84: 61 – 82

Masrouhi, A., Ghanmi, M., Ben Slama, M. M., et al., 2008. New Tectono-Sedimentary Evidence Constraining the Timing of the Positive Tectonic Inversion and the Eocene Atlasic Phase in Northern Tunisia: Implication for the North African Paleo-Margin Evolution. *Comptes Rendus Geoscience*, 340(11): 771 – 778. https://doi. org/10.1016/j.crte.2008.07.007

Mejri, F., Burollet, P. F., Ben Ferjani, A., 2006. Petroleum Geology of Tunisia. Mémoir de L'ETAP, Tunisia. 22: 233

Melki, F., Zouaghi, T., Ben Chelbi, M., et al., 2010. Tectono-Sedimentary Events and Geodynamic Evolution of the Mesozoic and Cenozoic Basins of the Alpine Margin, Gulf of Tunis, North-Eastern Tunisia Offshore. *Comptes Rendus Geoscience*, 342(9): 741 – 753. https://doi.org/10.1016/j.crte.2010.04.005

Menant, A., Jolivet, L., Vrielynck, B., 2016. Kinematic Reconstructions and Magmatic Evolution Illuminating Crustal and Mantle Dynamics of the Eastern Mediterranean Region since the Late Cretaceous. *Tectonophysics*, 675: 103–140. https://doi.org/10.1016/j.tecto.2016.03.007

Midassi, M. S., 1982. Regional Gravity of Tunisia: [Dissertation]. Univ. South Carolina. USA. 125

Min, G., Hou, G. T., 2019. Mechanism of the Mesozoic African Rift System: Paleostress Field Modeling. *Journal of Geodynamics*, 132: 101655. https://doi.org/10.1016/j.jog.2019.101655

Morgan, M. A., Grocott, J., Moody, R. T. J., 1998. The Structural Evolution of the Zaghouan-Ressas Structural Belt, Northern Tunisia. *Geological Society*, *London*, *Special Publications*, 132(1): 405 – 422. https://doi.org/10.1144/gsl.sp.1998.132.01.23

Nejia, L. O., Bédir, M., 2004. Les Migrations Tectono-Magmatiques du Trias au Miocène sur la Marge Orientale de la Tunisie. *Africa Geosciences Review*, 11(3): 179–196

Nikishin, A. M., Cloetingh, S. A. P. L., Brunet, M. F., et al., 1998. Scythian Platform, Caucasus and Black Sea Region: Mesozoic–Cenozoic Tectonic

History and Dynamics. In: Crasquin-Soleau, S., Barrier, E., eds., Peri-Tethys Memoir 3: Stratigraphy and Evolution of Teri-Tethyan Platforms, Paris. 163–176

Nikishin, A. M., Okay, A., Tüysüz, O., et al., 2015a. The Black Sea Basins Structure and History: New Model Based on New Deep Penetration Regional Seismic Data. Part 1: Basins Structure and Fill. *Marine and Petroleum Geology*, 59: 638–655. https://doi. org/610.1016/j. marpetgeo. 2014.1008.1017

Nikishin, A. M., Okay, A., Tüysüz, O., et al., 2015b. The Black Sea Basins Structure and History: New Model Based on New Deep Penetration Regional Seismic Data. Part 2: Tectonic History and Paleogeography. *Marine and Petroleum Geology*, 59: 656–670. https://doi.org/10.1016/j. marpetgeo.2014.08.018

Piqué, A., Ait Brahim, L., Ait Ouali, R., et al., 1998. Evolution Structurale des Domaines Atlasique du Maghreb au Méso-Cénozoïque: Le Rôle des Structures Héritées dans la Déformation du Domaine Atlasique de L'Afrique de Nord. *Bulletin de la Société Géologique France*, 169(6): 797–810

Piqué, A., Tricart, P., Guiraud, R., et al., 2002. The Mesozoic-Cenozoic Atlas Belt (North Africa): An Overview. *Geodinamica Acta*, 15(3): 185–208. https://doi.org/10.1080/09853111.2002.10510752

Platt, J. P., Behr, W., Johanesen, K., et al., 2013. The Betic-Rif Arc and Its Orogenic Hinterland: A Review. *Annual Review of Earth and Planetary Sciences*, 41: 313 – 357. https://doi. org/10.1146/annurev-earth-050212-123951

Raulin, C., de Lamotte, D. F., Bouaziz, S., et al., 2011. Late Triassic-Early Jurassic Block Tilting along E-W Faults, in Southern Tunisia: New Interpretation of the Tebaga of Medenine. *Journal of African Earth Sciences*, 61(1): 94–104. https://doi.org/10.1016/j.jafrearsci.2011.05.007

Rosenbaum, G., 2014. Geodynamics of Oroclinal Bending: Insights from the Mediterranean. *Journal of Geodynamics*, 82: 5–15. https://doi.org/10.1016/j.jog.2014.05.002

Rosenbaum, G., Lister, G. S., Duboz, C., 2002. Relative Motions of Africa, Iberia and Europe during Alpine Orogeny. *Tectonophysics*, 359(1/2): 117–129. https://doi.org/10.1016/s0040-1951(02)00442-0

Saïd, A., Baby, P., Chardon, D., et al., 2011. Structure, Paleogeographic Inheritance, and Deformation History of the Southern Atlas Foreland Fold and Thrust Belt of Tunisia. *Tectonics*, 30(6): TC6004. https://doi.org/10.1029/2011tc002862

Saïd, A., Chardon, D., Baby, P., et al., 2011. Active Oblique Ramp Faulting in the Southern Tunisian Atlas. *Tectonophysics*, 499(1/2/3/4): 178–189. https://doi.org/10.1016/j.tecto.2011.01.010

Sekatni, N., Fauré, P., Alouani, R., et al., 2008. Le Passage Lias-Dogger de la Dorsale de Tunisie Septentrionale. *Comptes Rendus Palevol*, 7(4): 185–194. https://doi.org/10.1016/j.crpv.2008.03.001

Soussi, M., 2003. New Jurassic Lithostratigraphic Chart for the Tunisian Atlas. *Geobios*, 36(6): 761–773

Soyer, C., Tricart, P., 1987. La Crise Aptienne en Tunisie Central: Approche Paléostructurale aux Confins de L'Atlas et de L'Axe Nord-Sud. *Comptes Rendus de l' Académie des Sciences Paris*, 305(II): 301–305

Stampfli, G. M., Borel, G. D., 2002. A Plate Tectonic Model for the Paleozoic and Mesozoic Constrained by Dynamic Plate Boundaries and Restored Synthetic Oceanic Isochrons. *Earth and Planetary Science Letters*, 196(1/2): 17–33. https://doi. org/10.1016/s0012-821x(01)00588-x

Tanfous Amri, D., Bédir, M., Soussi, M., et al., 2005. Halocinèse Précoce Associée au Rifting Jurassique Dans L'Atlas Central de Tunisie (Région de Majoura-El Hfay). *Comptes Rendus Geoscience*, 337(7): 703–711. https://doi.org/10.1016/j.crte.2005.02.007

Tlig, S., Er-Raoui, L., Ben Aissa, L., et al., 1991. Tectogenèses Alpine et Atlasique: Deux Evènements Distincts dans L'histoire Géologique de la Tunisie. Corrélation avec les Evènements Clés de la Méditerranée. *Comptes Rendus Académie de Sciences Paris*, 312(II): 295–301

Vila, J. M., Ben Youssef, M., Charrière, A., et al., 1994. Découverte en Tunisie au SW du Kef de Matériel Triasique Interstratifié dans L'Albien: Extension du Domaine à «Glacier de sel» Sous-Marin des Confins Algéro-Tunisiens. *Comptes Rendus Académie de Sciences Paris*, 318(II): 109–116

Vissers, R. L. M., Meijer, P. T., 2012. Iberian Plate Kinematics and Alpine Collision in the Pyrenees. *Earth-Science Reviews*, 114(1/2): 61–83. https://doi.org/10.1016/j.earscirev.2012.05.001

Ye, J., Chardon, D., Rouby, D., et al., 2017. Paleogeographic and Structural Evolution of Northwestern Africa and Its Atlantic Margins since the Early Mesozoic. *Geosphere*, 13(4): 1254–1284. https://doi.org/10.1130/ges01426.1

Yelles-Chaouche, A. K., Ait Ouali, R., Bracene, R., et al., 2001. Chronologie de L'ouverture du Bassin des Ksour (Atlas Saharien, Algerie) au debut du Mesozoique. *Bulletin de la Société Géologique de France*, 172(3): 285–293. https://doi.org/10.2113/172.3.285

Zouaghi, T., Bedir, M., Inoubli, M. H., 2005. 2D Seismic Interpretation of Strike-Slip Faulting, Salt Tectonics, and Cretaceous Unconformities, Atlas Mountains, Central Tunisia. *Journal of African Earth Sciences*, 43(4): 464–486. https://doi.org/10.1016/j.jafrearsci.2005.09.010

Zouaghi, T., Ferhi, I., Bédir, M., et al., 2011. Analysis of Cretaceous (Aptian) Strata in Central Tunisia, Using 2D Seismic Data and Well Logs. *Journal of African Earth Sciences*, 61(1): 38–61. https://doi.org/10.1016/j.jafrearsci.2011.05.002

Zouaghi, T., Inoubli, M. H., Bédir, M., 2007. Contribution of Seismic Velocity Studies to Structural and Lithostratigraphic Reconstructions: Salt-Intruded Corridor Ceiling and Lower Turonian Beida Anhydrite Deposits' Outline in the Central-Southern Atlas of Tunisia. *Comptes Rendus Geoscience*, 339(1): 13 – 23. https://doi. org/10.1016/j. crte. 2006.12.002

Zouari, H., Turki, M., Delteil, J., et al., 1999. Tectonique Transtensive de la Paléomarge Tunisienne au cours due L'Aptien-Campanien. *Bulletin de la Societe Geologique de France*, 170(3): 295–301